



# McGill

## **Closed Loop Control of Recycled HDPE Crosslinking Using an Inline Rheometer**

Antonio Pillo

Department of Chemical Engineering

McGill University

July 1993

A Thesis submitted to the Faculty of Graduate Studies and Research in partial fulfilment of the requirements of the degree of Master of Engineering.

© Antonio Pillo, 1993

Short title:

**Closed Loop Control of HDPE  
Crosslinking Using an Inline Rheometer**

## Abstract

This study involves the use of an inline rheometer (ILR) for process control. The ILR is a melt viscosity sensor that is mounted directly in the main process stream. This type of installation minimizes the measurement delay time, which is important for sensors used in process control applications.

The ILR was used for the closed loop control of product viscosity of post-consumer recycled high density polyethylene crosslinking in a twin screw extruder. The manipulated variable is the feed rate of crosslinking agent. Internal model control, Dahlin control, and minimum variance control algorithms were successfully implemented.

## Résumé

Cette étude concerne l'usage d'un rhéomètre en ligne (REL) utilisé en contrôle de procédé. Le REL est un capteur de viscosité de plastique fondu positionné directement dans le canal d'écoulement. Ce type d'installation minimise le retard de mesure du temps, qui est important pour les capteurs utilisés en contrôle de procédé.

Le REL a été utilisé pour le contrôle en boucle fermée de la viscosité de polyéthylène à haute densité recyclé soumis à une réticulation dans une extrudeuse à deux vis. La variable manipulée est la concentration de l'agent de réticulation. Des algorithmes de contrôle par modèle interne, par méthode de Dahlin, et par variance minimale ont été utilisés avec succès.

## Acknowledgements

I would like to thank my supervisors, Professors J.M. Dealy and W.I. Patterson, for their support and guidance throughout this project.

Burke Nelson provided a great deal of assistance throughout every aspect of this project.

Furong Gao helped me tremendously with process identification and control.

Luciano Cusmich, Charles Dolan, Jean Dumont, Alain Gagnon, Walter Greenland, and Mr. A. Krish provided much help in maintaining and modifying the extrusion facility.

I would like to thank Nabil Elkouh, Paul Lageraaen, Steve Helle, Bill McCaffrey, and Prof. D. Cooper for their friendship.

Michele, Maria, Robert, Teresa, Michael, and Julia have always been behind me.

Lastly, I would like to thank Dow Canada Ltd. for their support of this work in the form of advice and materials.

## Table of Contents

1. Introduction	1
1.1 Process Rheometry	1
1.1.1 Commercial Online Rheometers	1
1.1.2 Related Work	5
1.2 Recycled HDPE	8
2. Previous Work	9
2.1 Description of Rheometer and Control Loop	9
2.2 Effect of Pressure on SST	13
2.3 ILR Temperature Measurement and Control	15
2.4 Rheometer Motor	17
2.5 ILR Closed Loop Control	18
3. Modifications Made to ILR	21
3.1 Disk-Bar SST	21
3.2 Larger Rheometer Drum	23
3.3 Modification of the Temperature Measurement and Control Systems	23
3.4 DC Servomotor	25
4. Response of the Modified ILR	26
4.1 SST Output Noise Level	26
4.2 Pressure and Temperature Correction Model	27
4.3 SST Dead Weight Calibration	31
4.4 ILR Accuracy	34
5. Rheological Properties of Recycled HDPE	36
5.1 Variation Within Bulk Containers	36
5.2 Optimum Strain Rate	37
5.3 Arrhenius Temperature Correction Model	38
6. Closed Loop Control of HDPE Crosslinking	40
6.1 Data Acquisition and Control	40
6.2 System Identification by Step Response	42
6.3 IMC Controller Performance	50

6.4 Dahlin Controller Performance	54
6.5 Minimum Variance Controller Performance	57
6.6 Summary	59
7. Accomplishments and Recommendations	61
7.1 Summary of Accomplishments	61
7.2 Recommendations	61
7.2.1 Gravimetric Feeders	61
7.2.2 Large Pressure Drop in Rheometer	64
7.2.3 Control of Strain Rate	65
References	66
A1. Appendix of Experimental Procedures	68
A1.1 Typical Extruder Operating Conditions	68
A1.2 Preparation of Masterbatch	69
A1.3 Experimental Procedure	69
A2. Appendix of Software Listings	71
A2.1 PRBS System Identification Experiment Program	71
A2.2 Minimum Variance Control Program	75
A3. Appendix of Equipment Drawings	80
A3.1 Shear Stress Transducer CAD Analysis	80
A3.2 Shear Stress Transducer, Disk-Bar Detail	81
A3.3 Shear Stress Transducer, Disk-Bar Top View	82
A3.4 Shear Stress Transducer Housing	83
A3.5 Shear Stress Transducer, Active Face and Probe Target	84
A3.6 Rheometer Drum	85
A3.7 Gap Thermocouple	86
A3.8 DC Servomotor Mounting Bracket	87
A3.9 DC Servomotor Assembly Diagram	88

## List of Figures

Figure 1-1: Göttfert Bypass Rheograph	2
Figure 1-2: Göttfert Real Time Rheometer	3
Figure 1-3: Rheometrics On-Line Rheometer	4
Figure 1-4: Control System Used by Fritz and Stöhrer	5
Figure 1-5: Control System Used by Pabedinskas et al.	7
Figure 2-1a: Schematic Diagram of the Inline Rheometer, Side View CS	9
Figure 2-1b: Schematic Diagram of the Inline Rheometer, Top View CS	10
Figure 2-2: Control System Diagram	11
Figure 2-3: Control System Communication	12
Figure 2-4: Disk-Spring Shear Stress Transducer	13
Figure 2-5: Thermocouple Location	16
Figure 3-1a: Disk-Bar SST Beam Side CS	21
Figure 3-1b: Disk-Bar SST Beam Front CS	21
Figure 3-1c: Disk-Bar SST Beam Top CS	22
Figure 3-2: Gap Thermocouple Location	24
Figure 3-3: SST Temperature Control Elements	25
Figure 4-1: SST Output Signal Sampled at 100 Hz	26
Figure 4-2: Data Acquisition Technique	27
Figure 4-3: SST Response to Temperature	28
Figure 4-4: SST Response to Extruder Pressure	29
Figure 4-5: SST Response to Rheometer Temperature, Extruder Off	33
Figure 5-1: Variation Within Bulk Containers	36
Figure 5-2: Viscosity Curve for MFI 0.56 and 1.05 dg/min Resins	37
Figure 5-3: Activation Energy Versus Strain Rate for the MFI 1.05 dg/min Resin	39
Figure 6-1a: Frequency Response and Phase Lag of 3rd Order Butterworth Filter	41
Figure 6-1b: Frequency Response and Phase Lag of Averaging Filter	42
Figure 6-2: 0.03 % Peroxide Positive/Negative Step Change Response	43



Figure 6-3: Nelson's Rheometer Drum Cycle	44
Figure 6-4: Rheometer Drum Cycle	45
Figure 6-5: Step Response Using Cycle Shown in Figure 6-4	46
Figure 6-6: PRBS Response Test	47
Figure 6-7: Block Diagram of Stochastic Process Model	48
Figure 6-8: PRBS Response Test	49
Figure 6-9a: Viscosity Data for Setpoint Tracking Experiment Using Internal Model Control	51
Figure 6-9b: Peroxide Concentration Data for Setpoint Tracking Experiment Using Internal Model Control	51
Figure 6-10a: Viscosity Data for Setpoint Tracking Experiment Using Internal Model Control	53
Figure 6-10b: Peroxide Concentration Data for Setpoint Tracking Experiment Using Internal Model Control	53
Figure 6-11a: Viscosity Data for Setpoint Tracking Experiment Using Dahlin's Algorithm	55
Figure 6-11b: Peroxide Concentration Data for Setpoint Tracking Experiment Using Dahlin's Algorithm	55
Figure 6-12a: Viscosity Data for Load Rejection Experiment Using Dahlin's Algorithm	56
Figure 6-12b: Peroxide Concentration Data for Load Rejection Experiment Using Dahlin's Algorithm	56
Figure 6-13a: Viscosity Data for Setpoint Tracking Experiment Using Minimum Variance Control	58
Figure 6-13b: Peroxide Concentration Data for Setpoint Tracking Experiment Using Minimum Variance Control	58

## List of Tables

Table 4-1: Data Ranges for $P$ and $T$ Correction Model	30
Table 4-2: $P$ and $T$ Correction Model	30
Table 4-3: SST Calibration Model Parameters	34
Table 4-4: ILR Accuracy Results	35
Table 6-1: FOPDT Model Parameters for Step Changes	44
Table 6-2: FOPDT Model Parameters	48
Table 6-3: Discrete FOPDT With IMA Noise Model Parameters	50
Table 6-4: IMC Controller Tuning Parameters	52
Table 6-5: Summary of Closed Loop Control Results	59

## 1. Introduction

### 1.1 Process Rheometry

Viscosity measurements are commonly used to estimate the molecular weight of a polymer melt during production or processing. A manufacturer can track changes in product quality by monitoring the variation in viscosity of a product and make changes as necessary in order to improve the quality of its product.

However, these measurements are generally made offline at the present time, and disturbances in product viscosity can only be compensated for manually. An appropriate closed loop controller would reduce variations in product viscosity and thus quality by allowing quick automatic compensation for process disturbances.

#### 1.1.1 Commercial Online Rheometers

The sensor used in a control loop must have a response time that is short compared to the characteristic time of the process. This presents a difficulty in the case of polymer melts, since they are very viscous and flow velocities are therefore usually low, resulting in a large delay time before the melt reaches the measuring device. One type of commercial online rheometer, the Göttfert Bypass Rheograph, is shown in Figure 1-1.

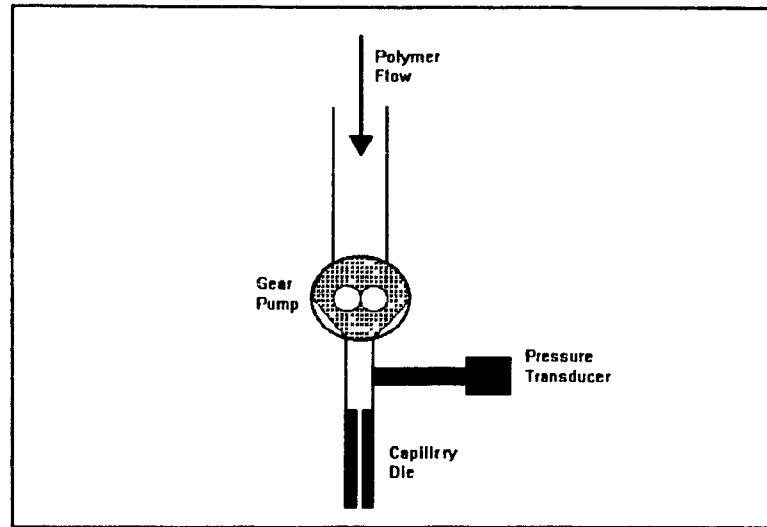


**Figure 1-1: Göttfert Bypass Rheograph**

This is a capillary type rheometer. A side stream leads to a gear pump which forces the melt through the capillary die, and a pressure transducer is used to measure the driving force. The shear stress  $\sigma$  can be calculated from the measured pressure drop across the die, and the apparent shear rate  $\dot{\gamma}_A$  can be calculated from the volumetric flow rate  $Q$  and the radius of the die  $R$ :

$$\dot{\gamma}_A \equiv \frac{4Q}{\pi R^3} \quad (1-1)$$

The apparent viscosity  $\eta_A$  can be calculated according to the definition:

$$\eta_A \equiv \frac{\sigma}{\dot{\gamma}_A} \quad (1-2)$$

Some finite amount of time is required for the melt to travel from the side stream entrance to the capillary die, as can be seen in the figure. This time is usually relatively large, since the flow rate through the die must be low. This results in a measurement delay time of 2 to 3 minutes at a strain rate of  $10 \text{ s}^{-1}$  [1].

Another type of commercial rheometer, the Göttfert Real Time Rheometer shown in Figure 1-2, can be used in order to decrease the measurement delay time.

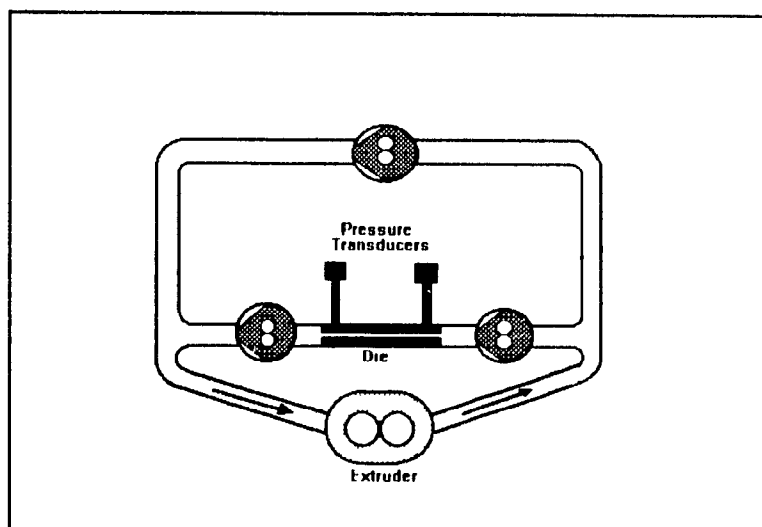


**Figure 1-2: Göttfert Real Time Rheometer**

This rheometer employs a gear pump for the sole purpose of maintaining a high flow rate in the sample loop in order to decrease the measurement delay time. This approach reduces the measurement delay time to 1 minute at a strain rate of  $10 \text{ s}^{-1}$  [1]. However, since the exit of the die is no longer at atmospheric pressure, this approach requires the addition of an extra gear pump and pressure transducer in order to make

the viscosity measurement. This complexity is undesirable from an industrial point of view, since maintenance requirements will increase. Additionally, both of the above rheometers share the drawback that gear pumps are unsuitable for use with highly filled polymer melts, limiting the potential applications for online viscosity measurement.

A different type of online rheometer is shown in Figure 1-3.

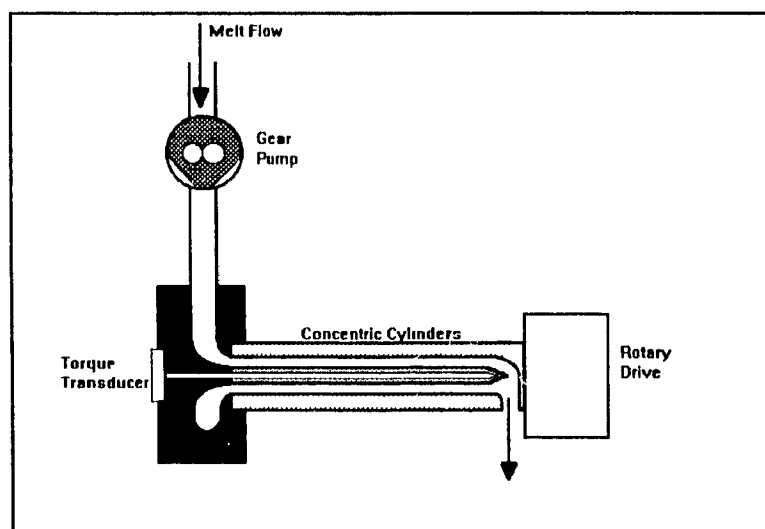


**Figure 1-3: Rheometrics On-Line Rheometer**

The Rheometrics On-Line Rheometer is of the rotational type. The polymer melt is pumped between concentric cylinders by means of a gear pump. The strain is caused by the oscillation of the outer cylinder, which is driven by the rotary drive. The resulting torque on the inner cylinder is measured by a torque tube transducer, which allows the shear stress to be calculated. This rheometer is most often used in a dynamic viscosity mode, which results in a longer measurement delay

than for a fixed strain rate, and adds to the dead time caused merely by conveying the melt to the concentric cylinders. Fritz and Stöhrer [2] reported a 3 minute process dead time attributed largely to the rheometer when operating at only high frequencies. In addition, this rheometer also has the disadvantage of requiring a gear pump.

### 1.1.2 Related Work

Fritz and Stöhrer [2] and Pabedinskas et al. [3] have studied closed loop control of reactive extrusion using online rheological measurement. Both studies involved polypropylene vis-breaking with organic peroxides.

A diagram of the control loop used by Fritz and Stöhrer is shown in Figure 1-4.

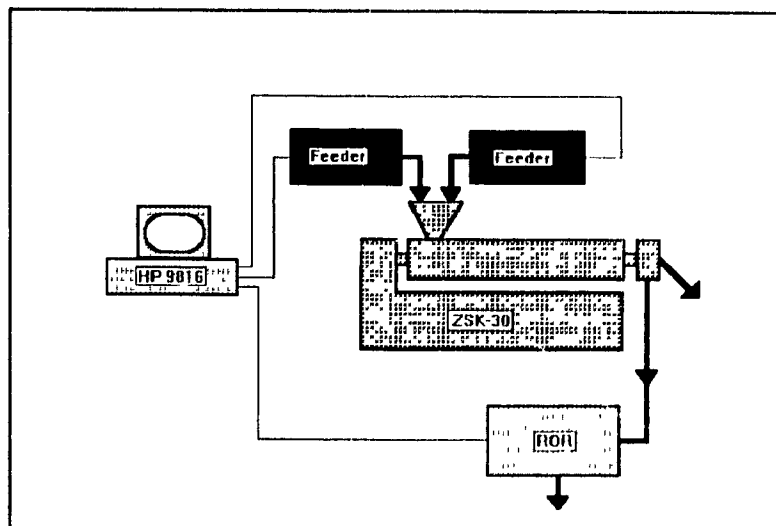


**Figure 1-4:** Control System Used by Fritz and Stohrer

A Rheometrics On-line Rheometer was used to monitor the dynamic viscosity. A computer sampled the rheometer signal and

calculated the required control action. It then implemented this control action by changing the feed rates of the two gravimetric feeders, one of which fed polypropylene and the other a peroxide masterbatch, while maintaining a constant total feed rate.

Fritz and Stöhrer used a first order plus deadtime (FOPDT) model fitted to step change tests in order to describe their process. They found a process dead time of 180 s and a time constant which was dependent on the direction of the step change. Positive steps in viscosity had a time constant of 156 s while negative steps had a time constant of 198 s.

Fritz and Stöhrer used proportional-integral (PI) control for closed loop experiments. Positive setpoint changes in viscosity exhibited an oscillatory response, with a settling time of 750 s. Negative setpoint changes exhibited a damped response, with settling times of 810 and 840 s. A load disturbance in which the masterbatch concentration was decreased from 0.2 % to 0.15 % yielded a settling time of 1500 s. A load disturbance in which the extruder screw speed was greatly increased resulted in a settling time of 600 s.

Pabedinskas et al. [3] used the control system shown in Figure 1-5.



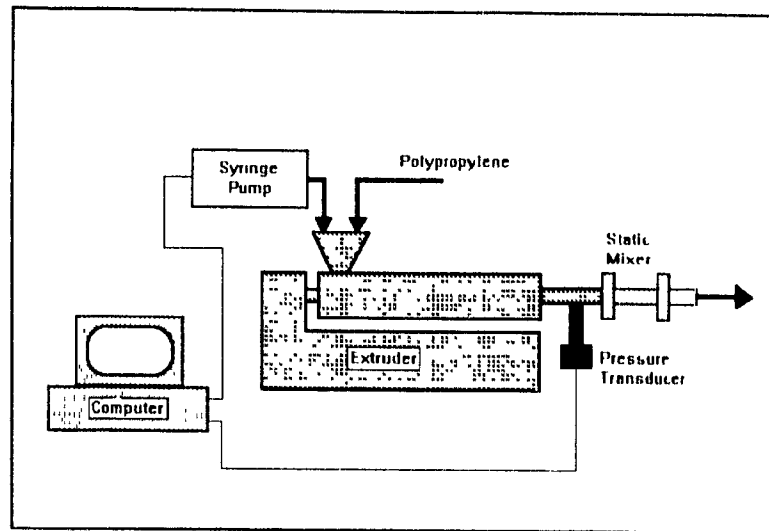


**Figure 1-5: Control System Used by Pabedinskas et al**

The pressure transducer and static mixer comprised a capillary type rheometer which made inline viscosity measurements. The computer sampled the calculated viscosity signal and calculated the required control action. The control action was implemented by changing the feed rate of the peroxide, which was fed by a syringe pump.

Pabedinskas et al. fitted a FOPDT model to step change tests to model their process. They found a process dead time of 160 s. Positive step changes in viscosity yielded time constants ranging from 112 to 165 s, and negative step changes yielded time constants from 95 to 146 s. The process gain was highly nonlinear, ranging from -58.5 MPa/% perox for a 0.04 % to 0.03 % step in peroxide concentration to -117.7 MPa/% perox for a 0.02 % to 0.01% step in peroxide concentration.

Pabedinskas et al. used a PI controller as well for their closed loop experiments. They obtained a response time of

900 s for setpoint changes, both with and without the use of gain scheduling. A load disturbance, caused by decreasing the pumping capacity of the syringe pump by one-third, resulted in a response time of 1920 s. Use of Smith Predictor control improved the closed loop response time for setpoint changes to 720 s.

## **1.2 Recycled HDPE**

A specific application that could benefit from closed loop control is the reprocessing of post-consumer, recycled, high density polyethylene (HDPE) currently carried out by Dow Canada in Ontario. Recycled material varies in quality and therefore presents a greater potential for causing fluctuations in product quality than virgin resin. A possible solution to this problem would be to partially crosslink the polyethylene in order to obtain a product stream of more uniform quality. Since viscosity can be used to indicate the degree of crosslinking, closed loop control of viscosity should reduce the variation in product quality.

Two post-consumer recycled HDPE resins of melt flow indices (MFI) 0.56 and 1.05 dg/min, supplied by Dow Canada, were used for this study. These are commercial resins that are presently used in blow molding applications where appearance and odour are not very important.

## 2. Previous Work

### 2.1 Description of Rheometer and Control Loop

A possible solution to the problem of slow sensor response discussed in section 1.1 would be to install the rheometer directly in the flow stream. This would shorten the path that the polymer melt would have to follow in order to reach the sensor and would thus reduce the response dead time. This would also circumvent the need for a positive displacement pump to deliver the melt to the sensor. The McGill inline rheometer (ILR) uses this approach.

The ILR is sketched in Figure 2-1.

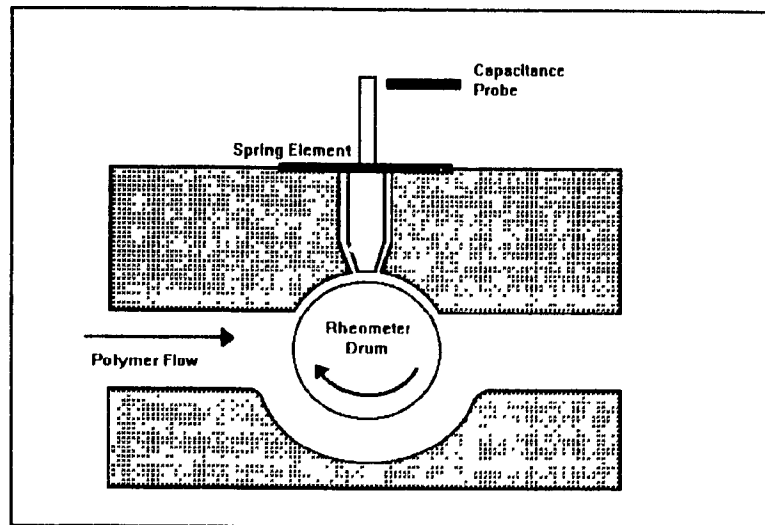


**Figure 2-1a:** Schematic Diagram of the Inline Rheometer, Side View CS

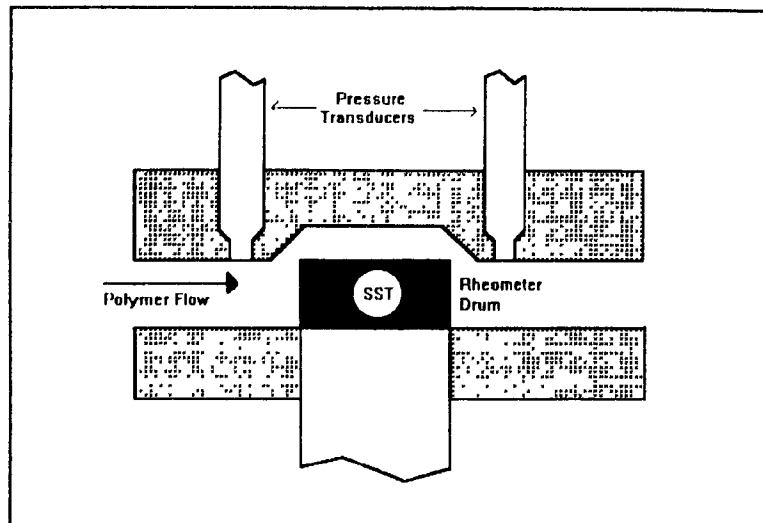


**Figure 2-1b:** Schematic Diagram of the Inline Rheometer, Top View CS

The rheometer drum drags melt into a narrow cylindrical gap formed between the rheometer housing and itself. The strain rate is related to the drum speed by:

$$\dot{\gamma} = \frac{\Omega R}{h} \quad (R \gg h) \quad (2-1)$$

where  $\Omega$  is the drum rotational speed (radians/s),  $R$  is the drum radius and  $h$  is the gap height. The shear stress at the wall  $\sigma$  is measured by means of a shear stress transducer (SST). The SST is composed of a rigid beam that pivots about a spring element and whose deflection is measured by means of a capacitance probe. Measurements can be made at various strain rates as indicated by equation 2-1.

The ILR is mounted at the exit of a Werner and Pfleiderer ZSK-30 co-rotating, intermeshing, twin-screw extruder,

directly in the main extrudate stream. The extruder barrel has an L/D ratio of 27 and is composed of four sections: (i) feeding and melting (ii) reaction (iii) devolatilization and (iv) pumping. The four sections have individual temperature control loops, with water cooling as well as electrical resistive heaters. A 250 W vacuum pump is connected to the devolatilization section via a cold trap.

The extruder and ILR have been used for several previous research projects. T.O. Broadhead [4] worked on the development of the rheometer and studied the control of ethylene methacrylic acid (EMAA) ionomer neutralisation in the extruder. T. Chen [6] studied the residence time distribution of the extruder alone and with the ILR. B.I. Nelson [7] also helped to develop the rheometer and studied control of polypropylene (PP) vis-breaking in the extruder.

The rheometer and extruder control system is sketched in Figure 2-2.

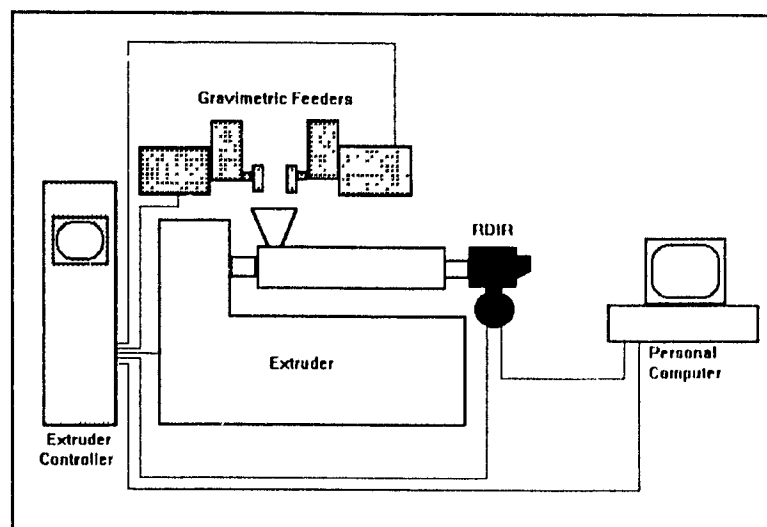


Figure 2-2: Control System Diagram

A Barber Colman MACO 8000 computer is used to control the extruder and the two Brabender DDSR 20 gravimetric feeders. A personal computer (PC) is used both to control the rheometer and to provide viscosity control, which is the outermost loop. One gravimetric feeder feeds resin, and the other a masterbatch containing Lupersol 101, a benzoyl peroxide-based crosslinking agent. The ratio of masterbatch to resin is changed, thereby changing the concentration of crosslinking agent in the feed, to compensate for deviations in melt viscosity while attempting to keep the overall mass flowrate constant.

A diagram that illustrates closed loop operation is shown in Figure 2-3.

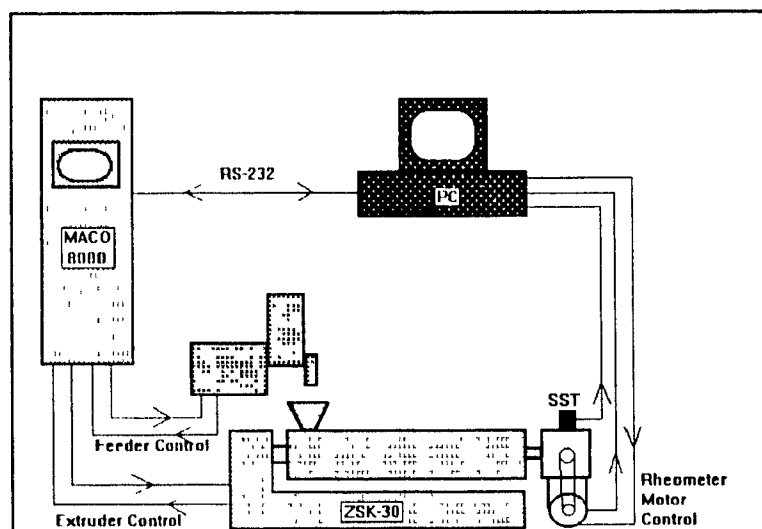


Figure 2-3: Control System Communication

The PC samples the rheometer signal and then calculates the required control action. It then communicates this information

to the MACO 8000. The MACO 8000 implements this control action by setting the feedrate of both gravimetric feeders (only one is shown). The MACO 8000 also provides control for the numerous loops nested within the viscosity control loop, such as extruder drive speed and temperature.

## 2.2 Effect of Pressure on SST

The SST beam was of the disk-spring type in the work of Broadhead [4] and Nelson [7], as shown in Figure 2-4.

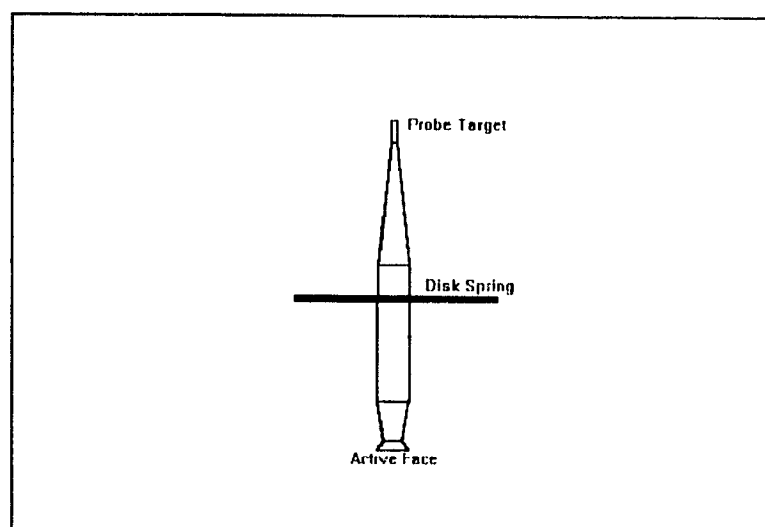


**Figure 2-4: Disk-Spring Shear Stress Transducer Beam**

This type of transducer beam is held in place by a thin stainless steel disk, which allows the beam to deflect under a shear stress at the active face, and which seals the upper part of the transducer body from the process stream. However, the flexibility of the disk also allows the beam to deflect axially in response to a normal stress. Therefore, pressure in the rheometer causes an axial deflection, which leads to false

indication of shear stress.

The extruder discharge pressure also affects the SST in another manner. Since the rheometer shearing gap is not isolated from the process stream, extruder pressure causes flow not only in the main rheometer flow channel but also in the shearing gap. Therefore, the true strain rate in the rheometer gap is not only a function of the drum speed but also of the pressure gradient along the gap. Most polymer melts are non-Newtonian, and determining the true strain rate in the rheometer gap is therefore not a trivial problem. Broadhead [4,5] developed a technique to correct for the effect of pressure flow on the shear rate profile across the rheometer gap.

For the simpler case where the rheometer drum is stationary, the wall shear stress for fully developed flow in a slit of negligible curvature and of height  $h$  and width  $w$  is related to the pressure drop  $\Delta P$  by:

$$\sigma = \frac{\Delta P h}{2L} \quad (2-2)$$

Nelson used a model of the following general form in order to correct for both the above mentioned pressure effects in the case where the rheometer drum is stationary:

$$\sigma (P_{rheometer}) = \beta_0 + \beta_1 P_{abs} + \beta_2 \Delta P \quad (2-3)$$

where  $P_{abs}$  refers to the absolute value of pressure at the



transducer, which is calculated by averaging the measurements from two pressure transducers placed equal distances upstream and downstream from the SST in the main rheometer flow channel.  $\Delta P$  is the difference between these two measurements.  $\beta_0$  is a constant which represents the shear stress caused by the rheometer drum along with the voltage offset of the probe amplifier. Nelson obtained values of 1.7 kPa(stress)/MPa(pressure) for  $\beta_1$  and 6.1 kPa(stress)/MPa(pressure drop) for  $\beta_2$  in his work using a polypropylene resin of MFI 2 dg/min and an SST calibration constant of 16 kPa/V. This value of  $\beta_2$  agrees reasonably well with the analytical result  $h/2L$  for fully developed flow in a slit with the dimensions of the rheometer gap.  $\beta_1$  is an empirical parameter.

### 2.3 ILR Temperature Measurement and Control

The viscosity of a polymer melt is a strong function of temperature. A commonly used temperature correction model is the Arrhenius equation:

$$\eta = \eta_0 \exp \left[ \frac{E_a}{R} \left( \frac{1}{T} - \frac{1}{T_0} \right) \right] \quad (2-4)$$

where  $E_a$  is the activation energy,  $R$  is the gas constant,  $\eta_0$  is the reference viscosity at the reference temperature  $T_0$ , and  $\eta$  is the corrected viscosity at temperature  $T$ . Both Broadhead [4] and Nelson [7] used this method.

A thermocouple placed within the metal of the rheometer

housing was used to estimate melt temperature  $T$  in the work of Broadhead and Nelson. This thermocouple was situated 13 mm upstream of the gap entrance and 9 mm above the flow channel, as indicated in Figure 2-5.

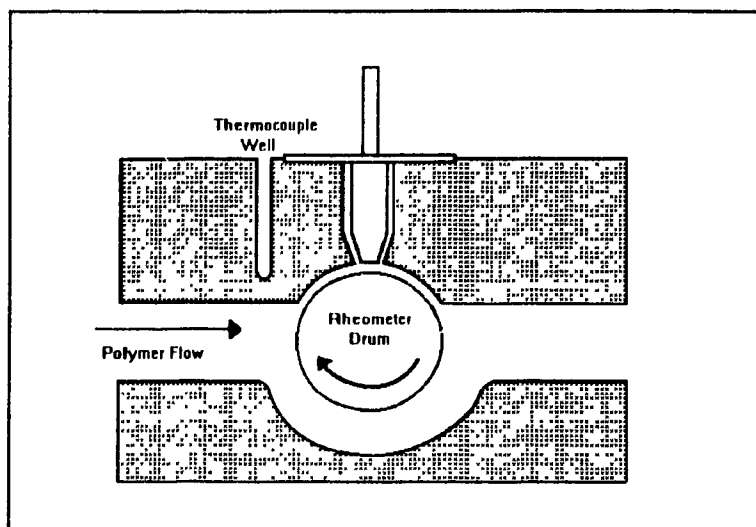


**Figure 2-5: Thermocouple Location**

There was some error in this method of temperature measurement, due to heat loss by conduction, and a time lag because of the thermal inertia of the metal, since the thermocouple was not in contact with the melt itself and was relatively far away from the gap.

Broadhead and Nelson also experienced problems in controlling the temperature of the SST itself. The temperature measurement used a washer thermocouple attached to the top of the SST housing, and a band heater was placed around the SST housing several centimetres below the thermocouple. They found that the control loop response was oscillatory, with an amplitude of 2 to 3°C when attempting to use the MACO 8000 in

autotuning mode and had to resort to manually selecting a heater duty cycle in order to avoid the deleterious effect of temperature cycling on the transducer response.

Broadhead fit a straight line for the SST output voltage versus the rheometer temperature over a temperature range of 180 to 210°C, without the extruder running, in order to quantify the effect of a temperature change on the SST response. He found a slope of  $-1.1 \text{ kPa}/^{\circ}\text{C}$  for a transducer calibration constant of  $16 \text{ kPa/V}$ .

#### **2.4 Rheometer Motor**

A 3/4 horsepower AC electric motor was used to rotate the rheometer drum through a 1:150 [output speed/input speed] gearbox in previous studies. However, this particular configuration presented some problems. The first was that output speed was not a linear function of the input voltage to the motor controller. This was solved by fitting a cubic polynomial to the relationship between motor speed and input voltage. The second was that viscosity measurements were made near the maximum motor speed (corresponding to  $30 \text{ s}^{-1}$ ), since this gave the best signal to noise ratio. If a higher drum speed had been attainable, this would possibly have resulted in both a better signal quality and a shorter rheometer response time.

## 2.5 ILR Closed Loop Control

Broadhead [4] implemented both integral time absolute error (ITAE) proportional-integral (PI) and minimum variance (MV) controllers in his work on closed loop control of EMAA neutralisation using the ILR. He fitted a first order plus dead time (FOPDT) model to the process, which in deviation variable form is:

$$\frac{\eta(t)}{C(t)} = K \left( 1 - e^{-\frac{t_d - t}{\tau}} \right) \quad (2-5)$$

where  $C$  represents the concentration of neutralising agent,  $K$  the process gain,  $t_d$  the process dead time, and  $\tau$  the process time constant. These were obtained from neutralising agent step change tests at a rheometer strain rate of  $30 \text{ s}^{-1}$ . Dead times in the range of 80 to 100 s and time constants ranging from 130 to 160 s were obtained for small viscosity steps.

Table 2-1 summarizes Broadhead's closed loop response time results for setpoint tracking using an ITAE PI controller design.

**Table 2-1:** Broadhead's Closed Loop Response Times for ITAE PI Control

Viscosity Step Size [Pa s]	Response Time [s]	
	Positive Steps	Negative Steps
60	320 to 360	250 to 290
120	430 to 540	300 to 325
200	515 to 530	318 to 320

Broadhead also performed load rejection experiments with PI control. He created load disturbances by changing to a masterbatch with a neutralising agent concentration 40 % lower than the initial value, and then changing back to the original value. These load disturbances at neutralisation setpoints of 15 and 22 % gave response times of 600 to 670 seconds.

Broadhead fitted a FOPDT model with an integrated moving average (IMA) noise model of the following form in order to implement minimum variance control:

$$\eta_t(z^{-1}) = \frac{\omega}{1-\delta z^{-1}} z^{-k} u_t + \frac{\theta}{(1-z^{-1})} a_t \quad (2-6)$$

where  $\omega$  is the discrete process gain,  $\delta$  the discrete process time constant,  $k$  the integer number of sampling periods per dead time,  $\theta$  the noise model parameter, and  $a_t$  the random noise. Using a sampling interval of 30 s, a dead time of 95 s, and a continuous process time constant of 130 s, Broadhead simulated the closed loop response to a 60 Pa s setpoint change. He obtained a response time of 255 s.

Nelson [7] studied the closed loop control of PP vis-

breaking and implemented both PI and minimum variance controllers. For PI control experiments, he first used an integral absolute error (IAE) PI controller based on a FOPDT process model with a dead time  $t_d$  of 56 s and a time constant  $\tau$  of 16 s. This controller achieved response times ranging from 50 to 320 seconds for 130-150 Pa·s steps in the viscosity setpoint at a strain rate of 30 s<sup>-1</sup>. However, the controller exhibited ringing.

He incorporated gain scheduling in order to compensate for the nonlinear process gain, and also a "gain factor" to compensate for the nonlinearity in the dynamic response of the process in order to refine the controller response. This resulted in improved response times ranging from 66 to 96 seconds for 120 Pa·s steps in the setpoint. Nelson also performed load rejection experiments with this controller by simulating a disturbance using the controller software. He achieved a response time of 225 seconds.

Nelson's implementation of minimum variance control incorporated two gain terms ( $\omega_0$  and  $\omega_1$ ) instead of the single term shown in equation 2-6, and also incorporated gain scheduling. Response times ranging from 70 to 230 seconds were achieved for 120 Pa·s steps in controller setpoint. Load rejection experiments in which the masterbatch concentration was halved and then changed back resulted in response times ranging from 225 to 290 s.

### 3. Modifications Made to ILR

#### 3.1 Disk-Bar SST

In order to reduce the effect of normal stress (pressure) on the shear stress measurement, a disk-bar type SST was designed by Sentmanat [8] and installed on the ILR. The SST beam is shown in Figure 3-1.

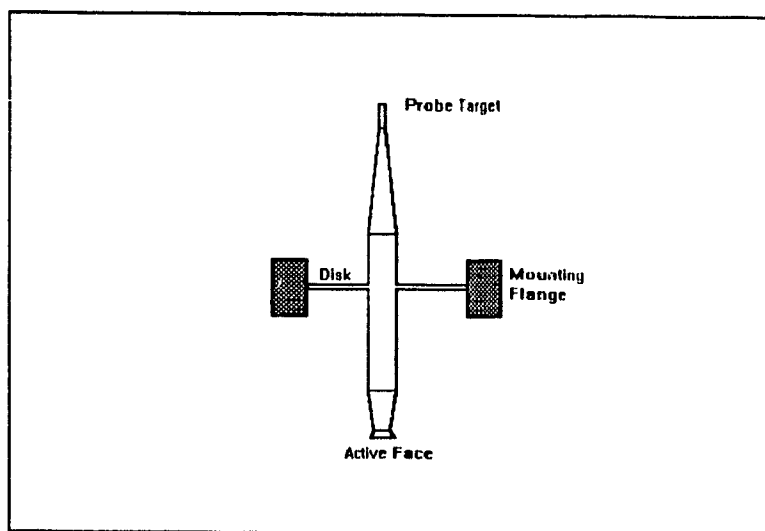


Figure 3-1a: Disk-Bar SST Beam Side CS

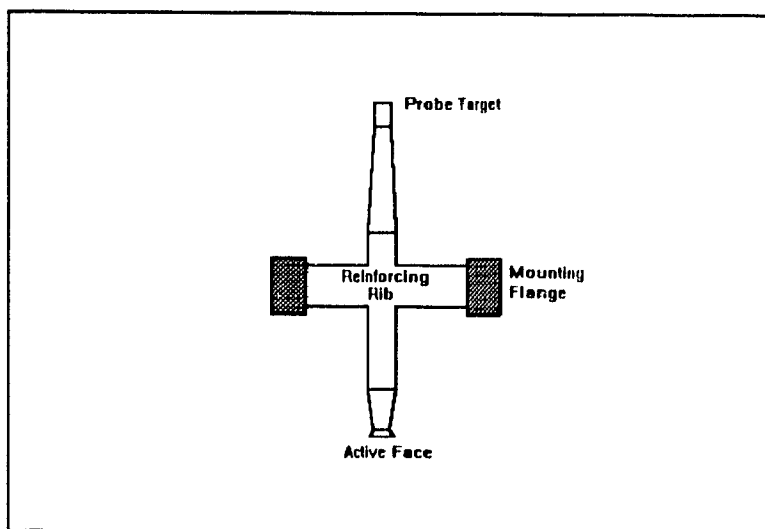
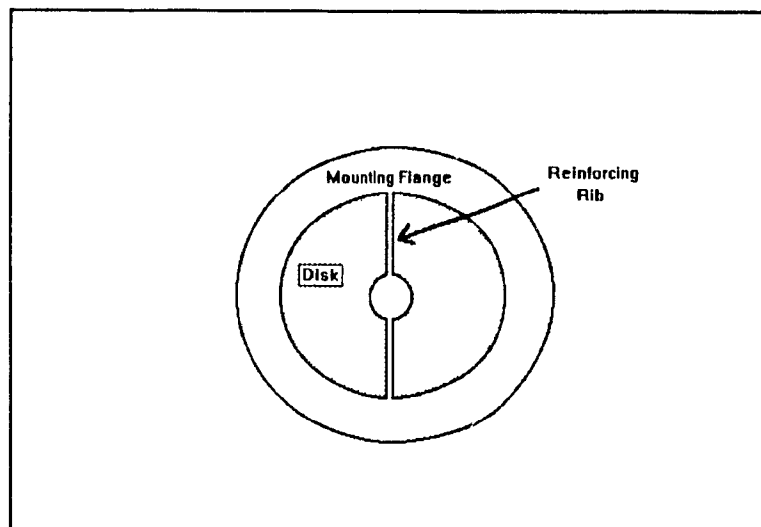


Figure 3-1b: Disk-Bar SST Beam Front CS



**Figure 3-1c: Disk-Bar SST Beam Top CS**

This device differs from the disk-spring SST beam in that the spring element incorporates a thin rectangular reinforcing rib. This rib is oriented parallel to the axis of drum rotation and serves to stiffen the disk against an axial force, yet allow it to flex sufficiently in response to a shear stress.

Both Broadhead [4] and Nelson [7] also experienced problems with the capacitance probe they used. The disk-spring SST was designed for an expected full scale deflection of 0.0254 mm at the probe. Broadhead used an MTI ASP-1HT probe and an Accumeasure System 1000 amplifier with a linear range of 0.0254 mm and a nominal gain of 10 V/0.0254 mm. This probe proved to be very difficult and time consuming to position because of its small linear range. For this reason, a Capacitec HPT-40 probe and 4100 amplifier with a linear range of 0.508 mm and the same nominal gain of 10 V/0.0254 mm was



chosen for the disk-bar SST.

### 3.2 Larger Rheometer Drum

The wall shear stress for pressure driven flow in a slit of height  $h$  and width  $w$  is given by equation 2-2:

$$\sigma_w = \frac{\Delta P h}{2L} \quad (2-2)$$

The corresponding flow rate for a Newtonian fluid is:

$$Q = \frac{h^3 w}{12\eta} \left( \frac{-\Delta P}{L} \right) \quad (3-1)$$

and the strain rate due to drum rotation is given by equation 2-1:

$$\dot{\gamma} = \frac{\Omega R}{h} \quad (R \gg h) \quad (2-1)$$

A reduction in gap height  $h$  for a given strain rate  $\dot{\gamma}$  and pressure drop  $\Delta P$  should therefore:

- i) reduce wall shear stress due to pressure flow
- ii) substantially reduce pressure flow
- iii) reduce the drum speed

For these reasons, the gap height was halved by increasing the drum diameter from 50 mm (used by Broadhead and Nelson) to 51 mm.

### 3.3 Modification of the Temperature Measurement and Control Systems

A Nanmac C8-5 Extrud-O-Couple was installed in the location shown in Figure 3-2 in order to reduce the error in

temperature measurement of the previous ILR configuration.

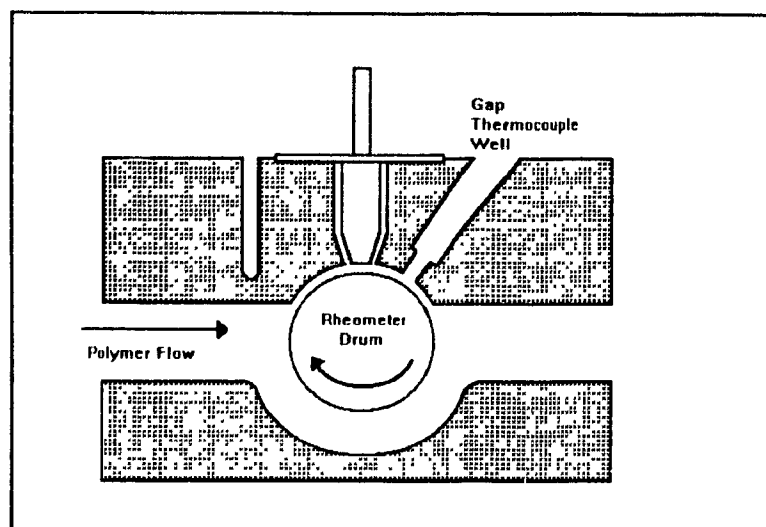


**Figure 3-2:** Gap Thermocouple Location

This E-type thermocouple has an exposed flat thermal junction at its surface which is insulated with ceramic in order to reduce heat conduction from the surrounding metal. An Omega DP41-TC temperature indicator with a resolution of  $0.01^{\circ}\text{C}$  was used to interface this thermocouple with the PC.

The new thermocouple and heater shown in Figure 3-3 were installed in order to improve control of the SST temperature.

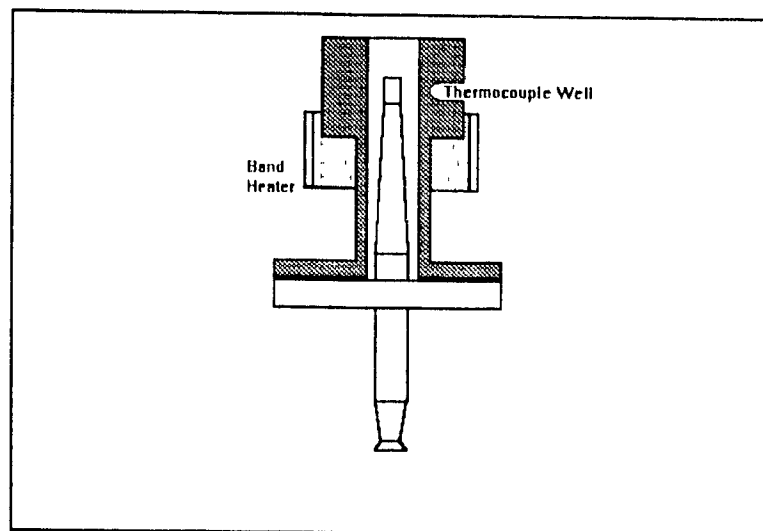


**Figure 3-3: SST Temperature Control Elements**

This serves to minimize the distance between the temperature sensor and the heater, and therefore minimizes the dead time in the temperature response. In addition, a sheet metal housing was built to fit around the rheometer and was filled with mineral wool to reduce the temperature gradients within the rheometer body.

### **3.4 DC Servomotor**

An Industrial Drives BR-2106-1011 DC Servomotor with PSR3 Power Supply and BDS3 Brushless Amplifier was installed in place of the 3/4 hp AC motor used previously in order to permit the use of a wider range of strain rates. Also, because of its internal motor speed control loop, the motor has a linear relationship between input voltage and output speed. This, together with the reduced gap, increased the maximum strain rate to  $185 \text{ s}^{-1}$ .

## 4. Response of the Modified ILR

### 4.1 SST Output Noise Level

A typical SST unfiltered output signal sampled at a frequency of 100 Hz at a strain rate of  $3 \text{ s}^{-1}$  is shown in Figure 4-1.

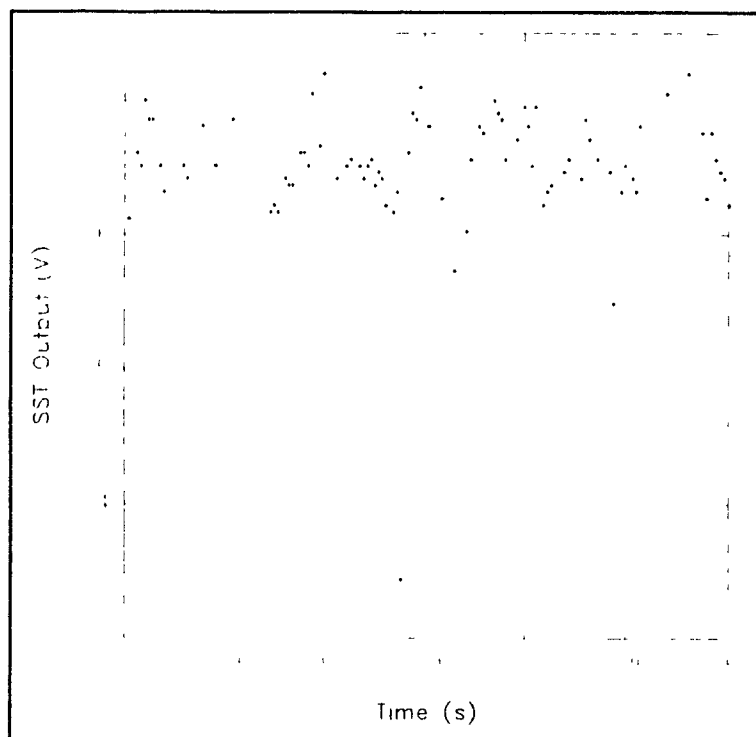


**Figure 4-1: SST Output Signal Sampled at 100 Hz**

This figure shows that the basic noise level from the SST when the extruder is in operation is approximately 100 mV peak to peak, for an SST calibration constant of 7.7 kPa/V, with occasional large spikes. This compares very well with the value of 80 mV experienced by Broadhead [4] for an SST calibration constant of 16 kPa/V, indicating that the modifications described in section 3 were collectively

successful.

#### 4.2 Pressure and Temperature Correction Model

Nelson [7] was forced to measure rheometer temperature before and after sampling pressure data and then to correct for any temperature drift in order to fit his pressure correction model. This was due to the fact that data obtained from the MACO 8000, to which the rheometer thermocouple is attached, are limited to a resolution of  $1^{\circ}\text{C}$  and a sampling rate on the order of 1 Hz. The addition of the gap thermocouple, which was interfaced directly to the PC, allowed data from different sensors to be sampled at a frequency of 25 000 Hz, allowing temperature and pressure data to be acquired simultaneously. The sampling technique is illustrated in Figure 4-2.

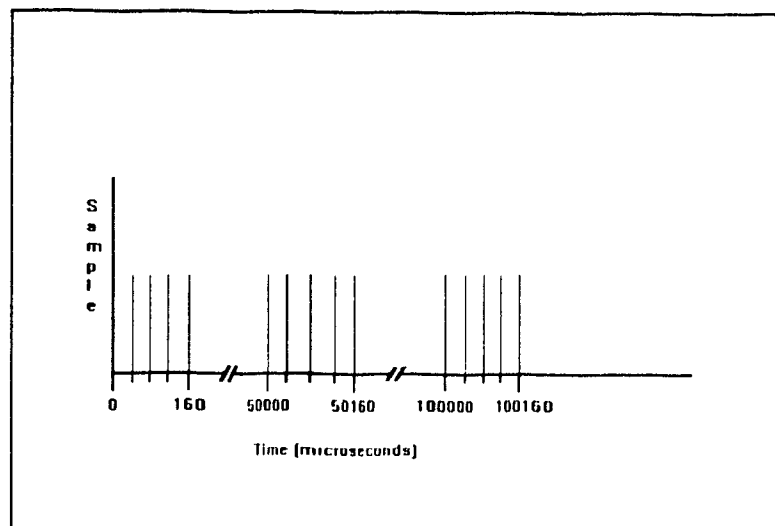
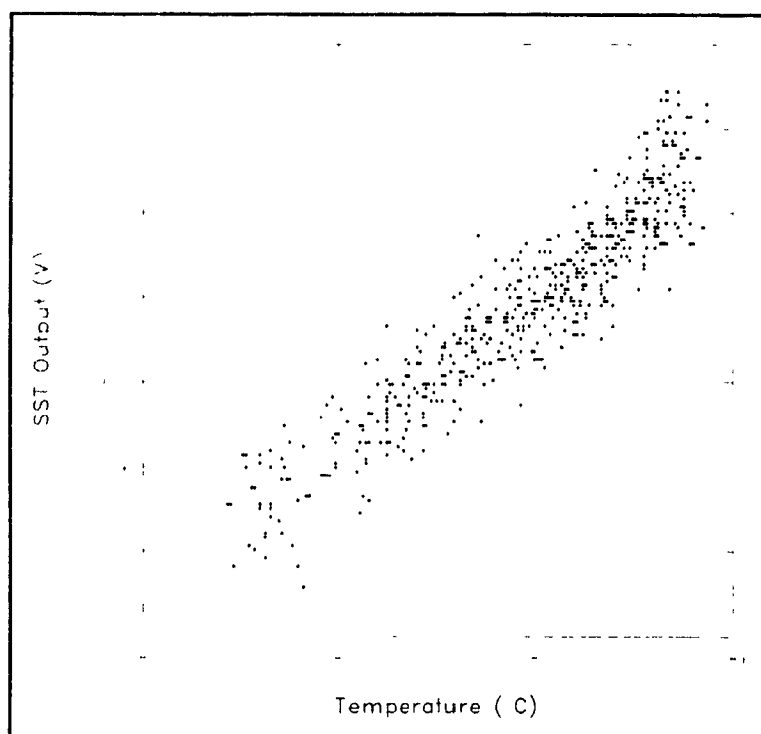


Figure 4-2: Data Acquisition Technique

The four input channels are sampled in rapid succession at

25 000 Hz, and then a pause of 0.05 s occurs, and the channels are sampled again, etc. Thus, the effective sampling rate for a given channel is 20 Hz, but the data from different channels is essentially simultaneous.

The variation of SST response with rheometer temperature is shown in Figure 4-3.



**Figure 4-3: SST Response to Temperature**

The data shown above are recorded from the startup transient occurring before the system has reached steady state and the rheometer drum is stationary. Contrary to the observation of Broadhead [4], these data indicate an increasing SST output with increasing temperature.

The variation of SST response with extruder pressure is shown in Figure 4-4.

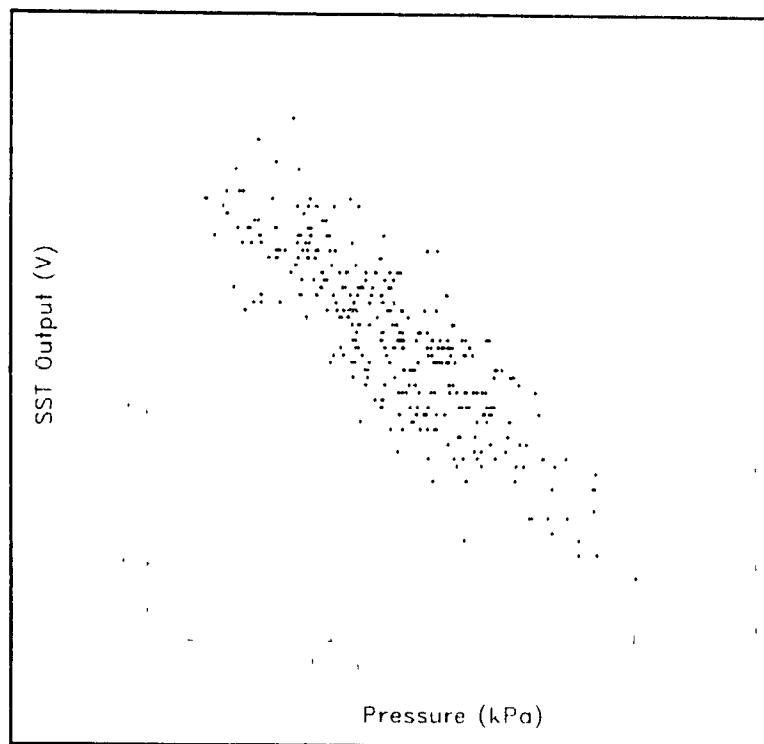


**Figure 4-4: SST Response to Extruder Pressure**

The above data are recorded from extruder operation at steady state. These data exhibit a negative slope, as observed by Broadhead and Nelson.

The pressure correction model was expanded to include a gap temperature correction term. A model of the form:

$$V_{SST} = \alpha_0 + \alpha_1 P_{abs} + \alpha_2 \Delta P + \alpha_3 T \quad (4-1)$$

was fitted using least squares regression on a one-half factorial experimental design. Data were collected for various combinations of exit die diameter, flowrate, and temperature. The range of values used for the model are shown in Table 4-1.

**Table 4-1: Data Ranges for  $P$  and  $T$  Correction Model**

30

Variable	Range
$P_{abs}$	1200-3800 kPa
$\Delta P$	220-820 kPa
$T_{gap}$	181-186 °C

The results are summarized in Table 4-2.

**Table 4-2:  $P$  and  $T$  Correction Model Parameters**

Parameter	Value	Std. Err.
$\alpha_1$ [V/MPa]	-0.165	0.00352
$\alpha_2$ [V/MPa]	0.426	0.0132
$\alpha_3$ [V/°C]	0.158	0.00116

For an SST calibration constant of 9.3 kPa/V, this corresponds to a stress correction of the following form:

$$\sigma(P_{rheo}, T_{gap}) = \beta_0 - 1.5 \frac{kPa}{MPa} P_{abs} + 4.0 \frac{kPa}{MPa} \Delta P + 1.5 \frac{kPa}{^\circ C} T \quad (4-2)$$

The pressure drop correction term coefficient (4.0) agrees only qualitatively with the theoretical value of 3.1 kPa(stress)/MPa(pressure drop). This lack of agreement is most probably due to the noise present in the measurements, which can easily be seen in Figures 4-3 and 4-4.



The severity of pressure and temperature effects on the SST output can be gauged by using typical operating ranges. The  $P_{abs}$  correction for a 700 kPa change in pressure is 1.0 kPa in the stress. The  $\Delta P$  correction for a 350 kPa change in pressure drop is 1.4 kPa in the stress. The temperature correction for a 0.6°C change in temperature is 0.9 kPa in the stress. Since the stress measurements were in the range of 20 to 40 kPa even at the low strain rate of 3 s<sup>-1</sup>, the pressure and temperature effects were judged to be negligible for this study, and data corrections were not performed, since obtaining a model for different operating conditions is very time consuming.

#### 4.3 SST Dead Weight Calibration

The SST was calibrated in place in the rheometer. The calibration involved suspending weights ranging from 50 to 300 g from the upper part of the transducer beam, utilizing an air bearing to negotiate the right angle turn. The effective shear stress at the active face that would cause a deflection of equal magnitude can be calculated and using also the measured SST voltage, the SST calibration constant can be calculated. This method implies two assumptions. The first is that the transducer beam is perfectly rigid. The effect of beam bending was shown to affect the calibration constant by only approximately 4 % by Sentmanat [8] for a disk-bar type SST and therefore was judged to be negligible for this

application.

The second assumption is that the SST response is symmetrical about the pivot axis. The clockwise rotation of the rheometer drum causes the beam target to move away from the capacitance probe, but a dead weight calibration method that could duplicate deflection of the beam in this direction is extremely difficult to implement due to interference from the extruder and rheometer housing itself. Sentmanat [8], by means of an external dead weight calibration, showed that the SST calibration constant of a disk-bar SST is independent of the direction of deflection.

Experimentation revealed that the SST calibration constant is a function of rheometer temperature. The variation of SST output voltage with rheometer temperature for a given beam deflection in the case where the extruder is not in operation is shown in Figure 4-5.

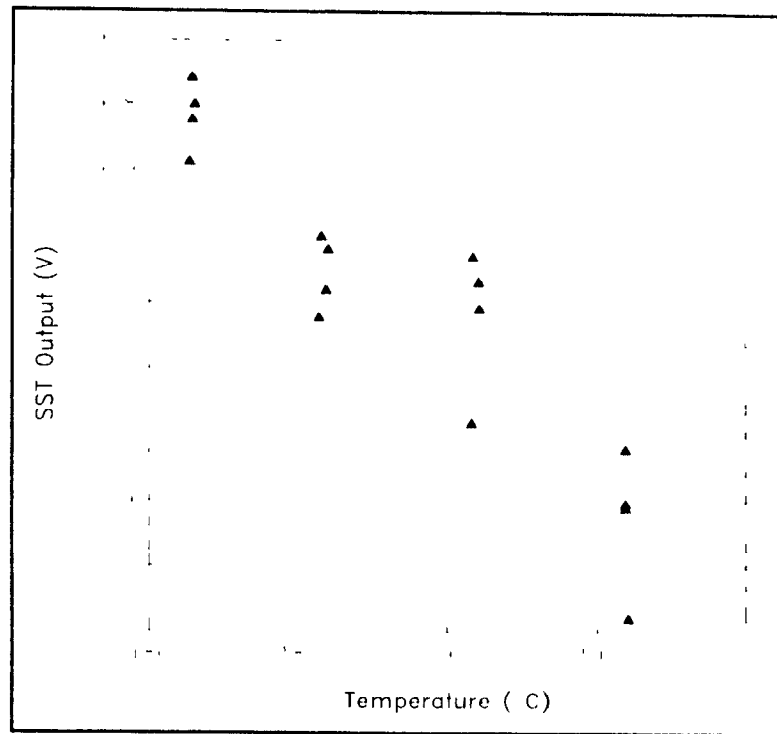


**Figure 4-5: SST Response to Rheometer Temperature, Extruder Off**

A model of the following form was fitted in order to correct for the effect of the rheometer temperature on the SST calibration constant:

$$\sigma = \delta_0 + \delta_1 V_{SST} + \delta_2 T \quad (4-3)$$

Effective shear stresses ranging from 17 to 52 kPa and temperatures ranging from 181 to 196°C were used to fit the model. The results are summarized in Table 4-3.

**Table 4-3: SST Calibration Model Parameters**

Parameter	Value	Std. Err.
$\delta_1$ [kPa/V]	-8.04	0.183
$\delta_2$ [kPa/°C]	-0.172	0.0585

The above values were used for the calculation of viscosity.

Since the gap thermocouple would physically interfere with the dead weight calibration apparatus, it was removed and the rheometer body thermocouple mentioned in section 2.3 used for temperature measurement for the model. However, as there was only one thermocouple amplifier available for data acquisition by the PC, the gap temperature was used in order to correct the SST calibration constant during actual experimentation using the extruder. This assumes that the gap temperature was the same as the rheometer body temperature during the modelling experiment, which is not strictly true, but because the extruder was not operating during this same experiment, the temperature difference between the rheometer gap and rheometer body was at least minimized.

#### **4.4 ILR Accuracy**

The ILR's accuracy was determined by comparing viscosity measurements between the ILR and the Rheometrics Dynamic Analyzer RDAII. Since the RDAII was used in dynamic viscosity mode, this comparison assumes that the resin obeys the Cox-

Merz rule:

$$\eta(\dot{\gamma}) = |\eta^*(\omega)| \quad (\omega = \dot{\gamma}) \quad (4-4)$$

Viscosity measurement results for the two rheometers are shown in Table 4-4.

**Table 4-4: ILR Accuracy Results**

Strain Rate [rad/s] or [s <sup>-1</sup> ]	Viscosity [kPa·s]	
	RDAII	ILR
3	9.7	9.2 std err = 0.025
5	7.2	6.7 std err = 0.045

These results are for the MFI 1.05 dg/min resin crosslinked with 0.03% peroxide. The ILR results agree with those of the RDAII within 7.5 %.

## 5. Rheological Properties of Recycled HDPE

### 5.1 Variation Within Bulk Containers

The Dow recycled HDPE is normally packaged in 500 kg Gaylord containers. Samples were taken from various corners of the box container in order to see if there is a significant variation in product viscosity within a container. Two replicate viscosity measurements of three different corner samples were then made using the Rheometrics Dynamic Analyzer RDAII. The results for both MFI 0.56 and 1.05 dg/min resins are shown in Figure 5-1.

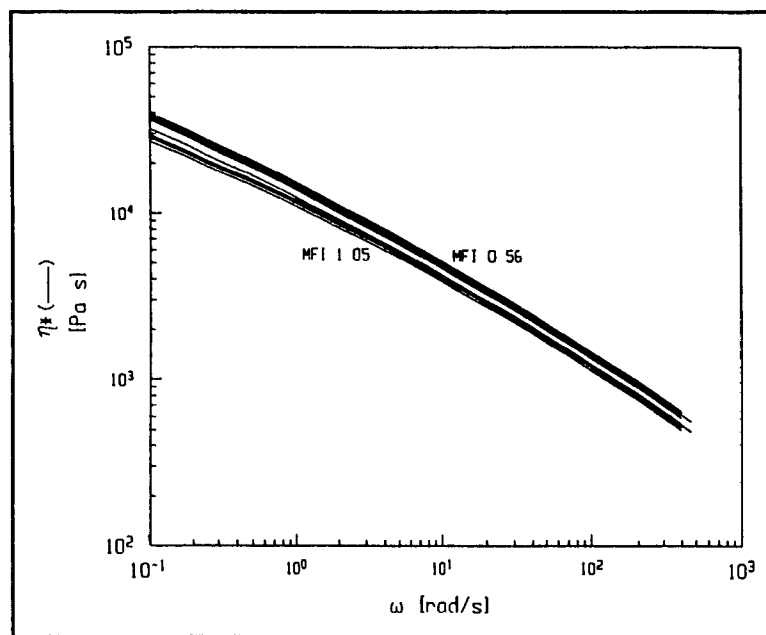


Figure 5-1: Variation Within Bulk Containers

The upper curve corresponds to MFI 0.56 dg/min and the lower to MFI 1.05 dg/min. The difference in viscosity between different samples was less than the error between replicates,

and therefore the viscosity of each grade of resin was considered constant.

## 5.2 Optimum Strain Rate

Based on the work of Broadhead [4] and Nelson [7], and also judging from commercial rheometer applications, strain rates ranging from 2 to 30  $\text{s}^{-1}$  are most suitable for online viscosity measurements. Viscosity data over this range for both MFI 0.56 and 1.05 dg/min resins are shown in Figure 5-2.

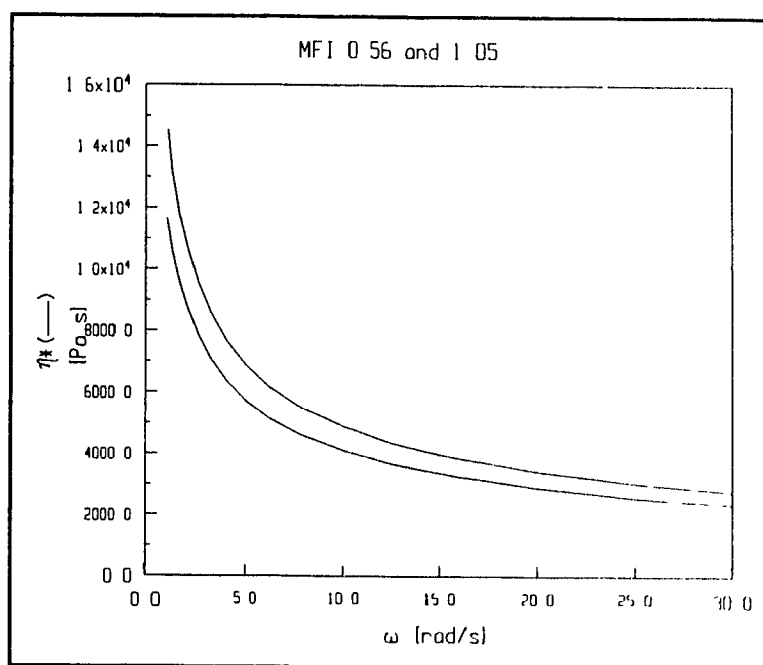


**Figure 5-2: Viscosity Curve for MFI 0.56 and 1.05 dg/min Resins**

The linear scale shows more clearly that the difference in viscosity between the two resins is larger at lower strain rates. However, use of low strain rates in the ILR would result in a larger uncertainty in the shear rate profile due

to pressure flow, a longer sample renewal time, and greater variance in the strain rate due to the motor/gearbox performance characteristics. Higher strain rates improve these problems, but the difference in viscosity is smaller at the higher strain rates, decreasing the signal to noise ratio. The strain rates that were used for online viscosity measurements were selected based on trial and error optimization of these factors. Since extrudate material properties other than viscosity were not measured for these resins, it was assumed that a viscosity signal resolution sufficient for successful closed loop control is also sufficient to resolve other important material properties more directly related to product quality.

### **5.3 Arrhenius Temperature Correction Model**

Since the strain rates that are of interest for viscosity measurement and control lie within the transition zone of the viscosity curve, the activation energy  $E_a$  used in the Arrhenius equation (2-4) is a function of strain rate. A graph of activation energy versus strain rate is shown in Figure 5-3.



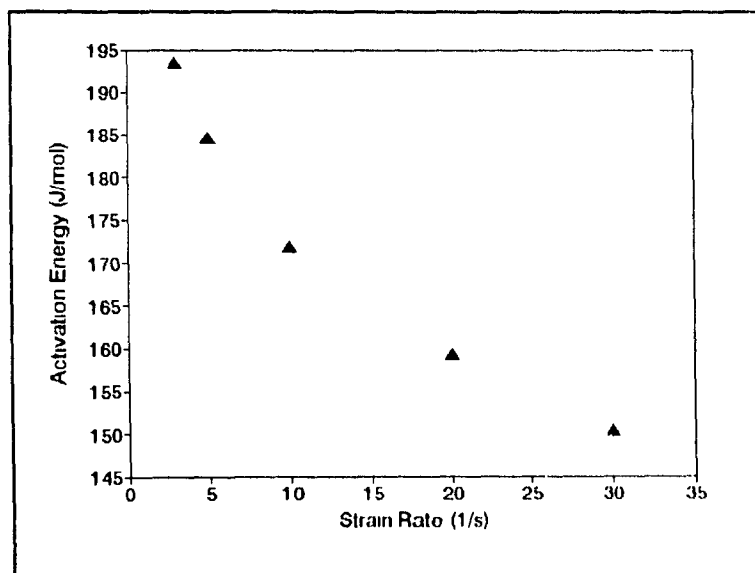


**Figure 5-3: Activation Energy Versus Strain Rate for the MFI 1.05 dg/min Resin**

These values were calculated from RDAII data over a temperature range of 176 to 205°C and were used in the correction for temperature changes during an ILR experiment.

## 6. Closed Loop Control of HDPE Crosslinking

### 6.1 Data Acquisition and Control

Data acquisition and control were implemented through the use of a PC with a Data Translation DT2801-A data acquisition card together with a Barber Colman MACO 8000 dedicated controller. The programming language used was Microsoft QuickBASIC 4.5, making use of many data acquisition routines, MACO serial communication routines, and a PRBS generating routine written by B.I. Nelson [9].

The general program structure is as follows:

- i) Wait until the extruder and rheometer have reached steady state.
- ii) Halt rheometer drum. Wait for polymer in gap to relax. Sample SST baseline voltage.
- iii) Begin rotating rheometer drum.
- iv) Sample SST measurement voltage and gap temperature. Calculate viscosity and correct for temperature fluctuation.
- v) Perform supervisory control action. Graph results.
- vi) Pause for the required time. Go to step iv).

Digital filtering was employed to reduce the effect of measurement noise. Since the PC had ample speed for supervisory control of viscosity, it was also used to implement software digital filtering techniques. The sampling and filtering technique used for data acquisition was as follows:

- i) Sample the 5 analog inputs at a sampling frequency of 100 Hz for 2 seconds.
- ii) Filter each set of 200 samples using a third order Butterworth, low pass filter with a corner frequency of 2.5 Hz.
- iii) Discard the first 100 samples to remove the filter startup transient.
- iv) Average the second 100 samples in order to obtain one datum.

This proved to be very effective in removing the 60 Hz AC line component of the measurement noise. The frequency response and phase lag of the two filters is shown in Figure 6-1.

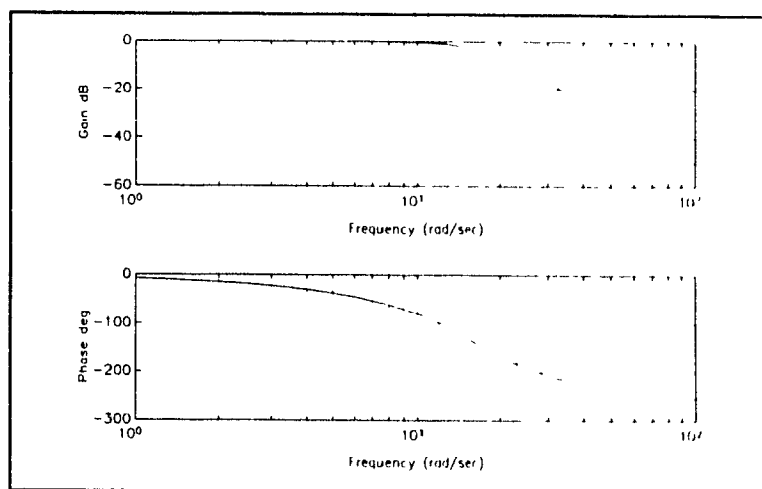


**Figure 6-1a:** Frequency Response and Phase Lag of 3rd Order Butterworth Filter

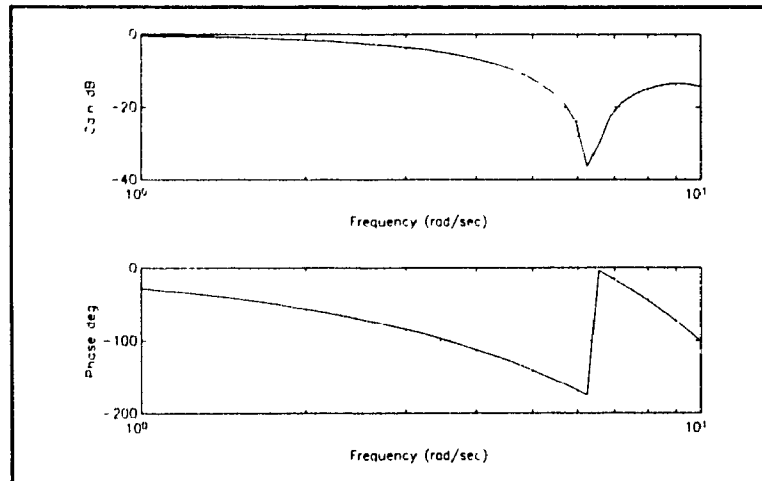


**Figure 6-1b: Frequency Response and Phase Lag of Averaging Filter**

The 3 dB attenuation points for both filters occur at frequencies greater than 1 Hz, and therefore the effect of the filters were judged to be negligible as compared to the dynamics of the process response.

## 6.2 System Identification by Step Response

Broadhead [4] and Nelson [7] found that the system consisting of the extruder plus rheometer exhibited an asymmetrical response to positive step versus negative step changes in reactant concentration. The same phenomenon was observed in the present study. A typical step up/step down experiment for MFI 1.05 recycled HDPE being crosslinked by Lupersol 101 at a strain rate of  $5 \text{ s}^{-1}$  and a temperature of  $194^\circ\text{C}$  is shown in Figure 6-2.

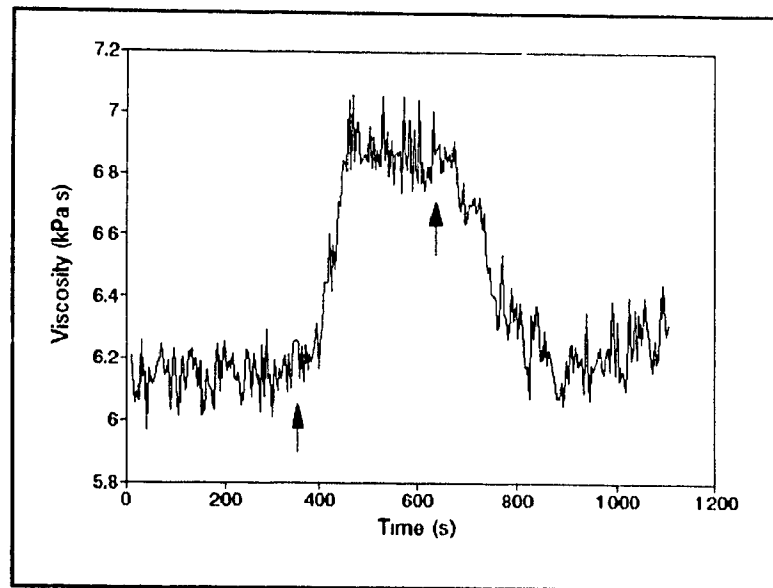


**Figure 6-2: 0.03 % Peroxide Positive/Negative Step Change Response**

The response is asymmetric in that the viscosity changes to the new level more rapidly during the positive step than the negative step, and also in that the process does not reach the same viscosity level after the step changes as before. This asymmetry causes difficulty in the fitting of a first order plus deadtime model to the process, since fitting a single model to both the positive and negative step responses causes a large uncertainty in the model. In addition, the degree of reproducibility of single step tests was poor. For a FOPDT model of the following form:

$$\frac{\eta(s)}{C(s)} = \frac{Ke^{-t_d s}}{\tau s + 1} \quad (6-1)$$

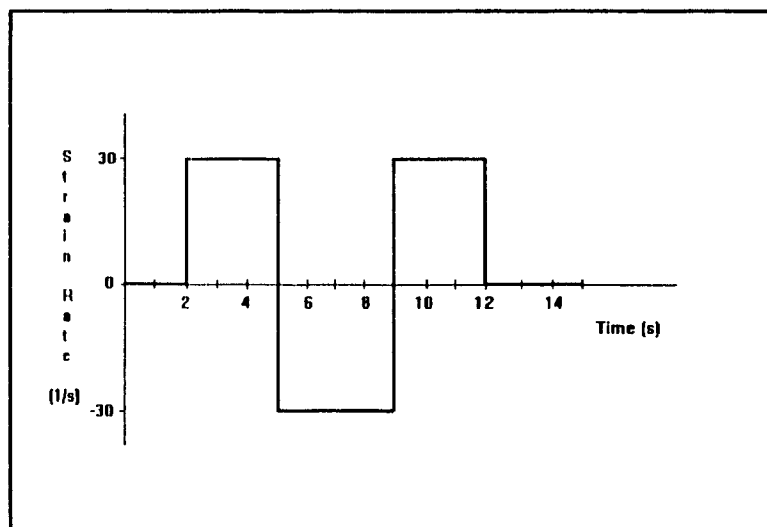
the following model parameters were obtained for step changes on the order of 1 kPa·s:

**Table 6-1: FOPDT Model Parameters for Step Changes**

Model Parameter	Step Change	
	Positive	Negative
$K$ [kPa s/% perox]	6.5 to 7.2	6.4 to 6.7
$\tau$ [s]	20 to 60	40 to 80
$t_d$ [s]	40 to 80	40 to 80

These model parameters were calculated using a FOPDT model fitting routine written by W.I. Patterson making use of the **FMINS** function of MATLAB 3.5 [10].

Nelson obtained shorter response times than Broadhead, which was attributed to his use of a drum rotation cycle which changed the direction of drum rotation during one sampling interval. His sampling cycle is shown in Figure 6-3.

**Figure 6-3: Nelson's Rheometer Drum Cycle**

He attributed this improvement in rheometer response time to the breaking up of eddies at the entrance to the rheometer

gap.

The use of similar rheometer drum cycles was studied during this work. One such cycle is shown in Figure 6-4.

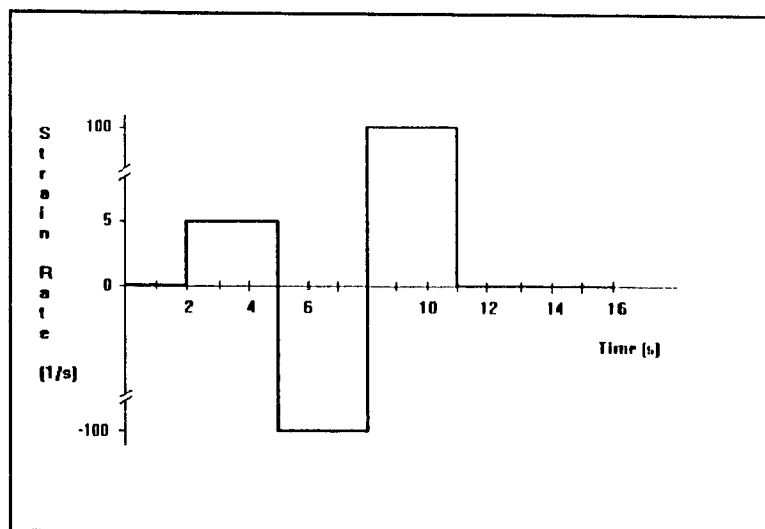


**Figure 6-4:** Rheometer Drum Cycle

This cycle yielded a step response as shown below:

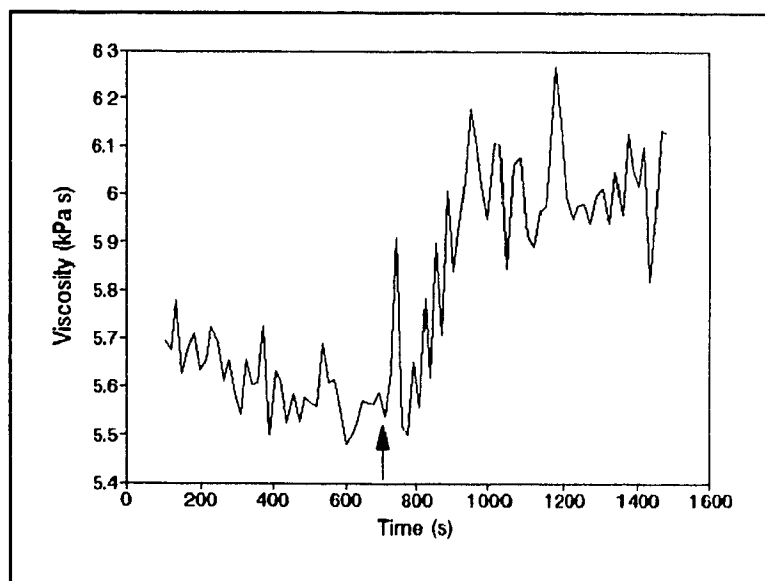


**Figure 6-5:** Step Response Using Cycle Shown in Figure 6-4

These results are for a 0.031 % step in peroxide concentration

in the MFI 1.05 dg/min material at a temperature of 180°C. The use of this type of rheometer cycling did improve response times in general, often lowering the first order time constant to a value in the range of 20-30 s. However, the deleterious effect of the rheometer cycle on the viscosity resolution is quite obvious when comparing Figure 6-5 to Figure 6-2. This is probably due to the large variation in pressure drop along the rheometer which occurs by alternating the direction of drum rotation. As discussed in Section 2.2, the rheometer pressure adversely affects the SST response, and rheometer cycling appears to aggravate this problem. Since this effect was very pronounced at the lower strain rates used in this study as compared to Nelson, rheometer cycling was not used, and the rheometer drum was rotated continuously at a single speed.

Nelson successfully used pseudo random binary sequence (PRBS) response tests in order to improve the degree of reproducibility of his process models. PRBS's are approximations to periodic white noise which consist of several or more step changes, and in the most basic sense can improve model accuracy merely by increasing the amount of data to which the model is fitted. In the present study, PRBS tests were also found to provide more reliable model parameters for the recycled HDPE crosslinking system. The results of a 4 stage PRBS response test for a 0.03% peroxide step at a strain rate of  $3 \text{ s}^{-1}$ , a sampling period of 8 s, and a temperature of 194°C is shown in Figure 6-6.



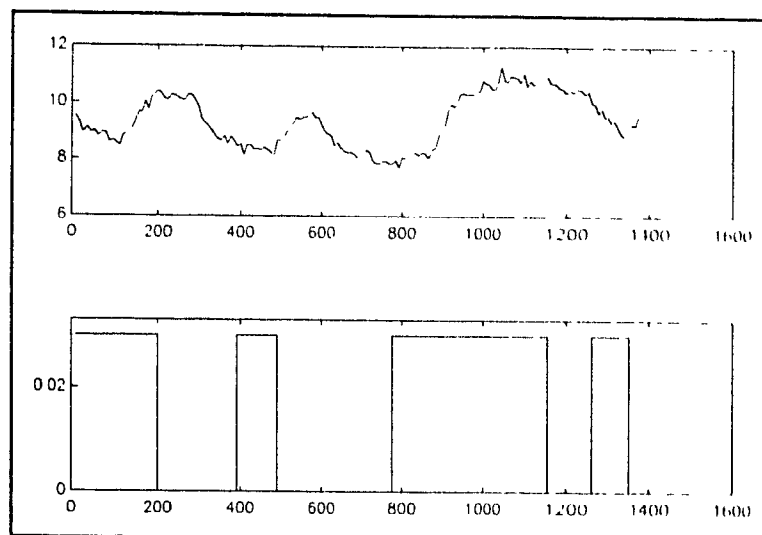


**Figure 6-6: PRBS Response Test**  
(units are kPa·s, % peroxide, and seconds)

A strain rate of  $3 \text{ s}^{-1}$  was used since preliminary closed loop experiments had shown that the poor resolution of the viscosity signal at  $5 \text{ s}^{-1}$  lead to poor controller response.

Both deterministic and stochastic process models were fitted to PRBS response test data. For the former, a discrete FOPDT model of the following form was fitted:

$$\eta_t(z^{-1}) = \frac{\omega}{1 - \delta z^{-1}} z^{-k} C_t \quad (6-2)$$

The model was fitted to the data using the **ARX** function of MATLAB System Identification Toolbox [11,12]. The **ARX** function fits a general model of the form:

$$A(q) y(t) = B(q) u(t-nk) + e(t) \quad (6-3)$$

using the least squares method. Using a strain rate of  $3 \text{ s}^{-1}$  and a sampling interval of 8 s with the MFI 1.05 dg/min material, the following values were obtained using a 4 stage

PRBS test:

**Table 6-2:** FOPDT Model Parameters

Parameter	Value	Std. Err.
$\omega$	9.98 [kPa·s]	1.05
$\delta$	0.880 [% perox]	0.0163
$k$	12	-

A block diagram of a stochastic model of the process is shown in Figure 6-7.

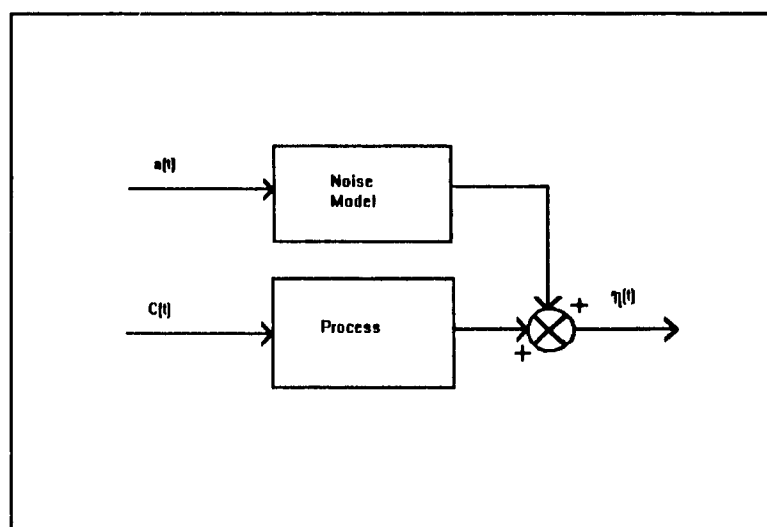


**Figure 6-7:** Block Diagram of Stochastic Process Model

A FOPDT process model with integrated moving average (IMA) noise model was fitted to the process. The IMA model is of the nonstationary type and is well suited to modelling a process where the mean level of the process drifts, yet apart from this drift any part of the series resembles any other part.

The model is shown below:

$$\eta_t(z^{-1}) = \frac{\omega}{1-\delta z^{-1}} z^{-k} C_t + \frac{1-\theta z^{-1}}{1-z^{-1}} a_t \quad (6-4)$$

where  $a_t$  represents the white noise. The corresponding PRBS data for the above model are shown in Figure 6-8.

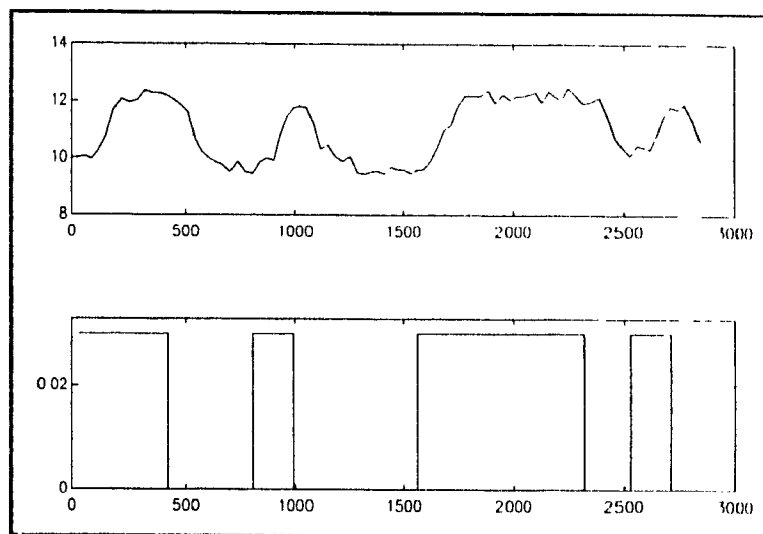


**Figure 6-8: PRBS Response Test**  
(units are kPa·s, % peroxide, and seconds)

This model was fitted using the **PEM** function of MATLAB. The **PEM** function fits a general model of the form:

$$A(q)y(t) = \frac{B_1(q)}{F_1(q)}u_1(t-nk_1) + \dots + \frac{B_{nu}(q)}{F_{nu}(q)}u_{nu}(t-nk_{nu}) + \frac{C(q)}{D(q)}e(t) \quad (6-5)$$

using a prediction error method. This function is used specifically because any of the parameters may be specified in advance, and if  $D(q)$  is fixed as  $(1-z^{-1})$ , a PI type minimum variance control equation can be derived. Using a strain rate of  $3 \text{ s}^{-1}$ , a sampling interval of 32 s, and at a temperature of  $196^\circ\text{C}$ , the following results were obtained for a 4 stage PRBS:

**Table 6-3: Discrete FOPDT With IMA Noise Model Parameters**

Resin	$\omega$ [kPa·s]	$\delta$ [% perox]	$\theta$ [kPa·s]	k
0.56 feed 0.56 MB	25.7 $\sigma=1.69$	0.717 $\sigma=0.0270$	0.525 $\sigma=0.0891$	3
0.56 feed 1.05 MB	22.6 $\sigma=1.67$	0.677 $\sigma=0.0343$	0.408 $\sigma=0.102$	3
1.05 feed 0.56 MB	29.5 $\sigma=1.90$	0.676 $\sigma=0.0290$	0.506 $\sigma=0.0943$	3
1.05 feed 1.05 MB	26.8 $\sigma=1.66$	0.707 $\sigma=0.0260$	0.577 $\sigma=0.0790$	3

### 6.3 IMC Controller Performance

Internal Model Control (IMC) is a control strategy that explicitly takes model uncertainty into account and also features an adjustable parameter to balance closed loop performance against controller robustness. Its form can be easily adjusted to provide conventional proportional-integral-derivative (PID) tuning relations for a wide variety of process models, including the FOPDT model used in this study. The continuous PID controller equation is:

$$C(s) = K_c \left( 1 + \frac{1}{\tau_I s} + \tau_D s \right) \eta(s) \quad (6-6)$$

and the IMC tuning parameters are:

$$K_c = \frac{1}{K} \frac{2 \left( \frac{\tau}{t_d} \right) + 1}{2 \left( \frac{\lambda_c}{t_d} \right) + 1} \quad \tau_I = \frac{t_d}{2} + \tau \quad \tau_D = \frac{\tau}{2 \left( \frac{\tau}{t_d} \right) + 1} \quad (6-7)$$

where  $\lambda_c$  is the closed loop time constant, which is the adjustable parameter. The discretized form of this controller is shown in Seborg et al. [13].

Early attempts at closed loop experimentation made use of process models obtained by averaging the results from both positive step and negative step experiments in order to obtain a single model. Some results obtained using this approach are shown in Figure 6-9.

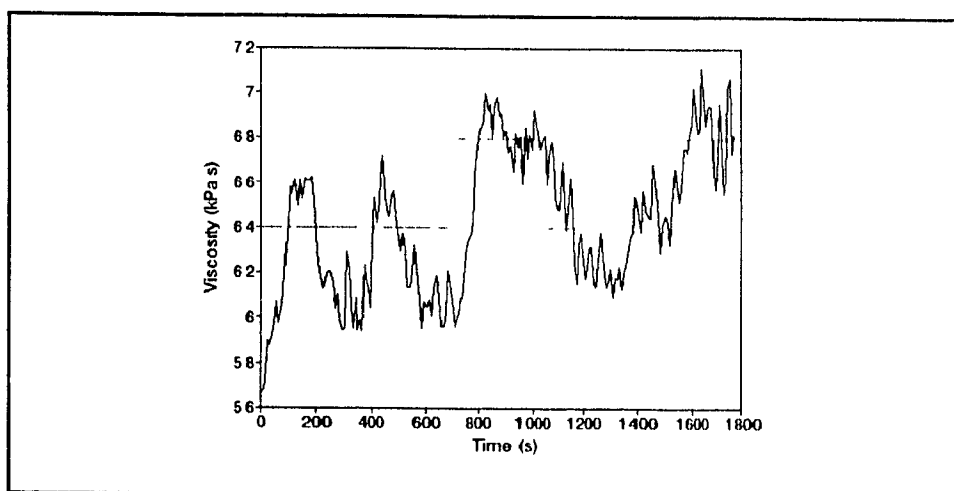


**Figure 6-9a:** Viscosity Data for Setpoint Tracking Experiment Using Internal Model Control

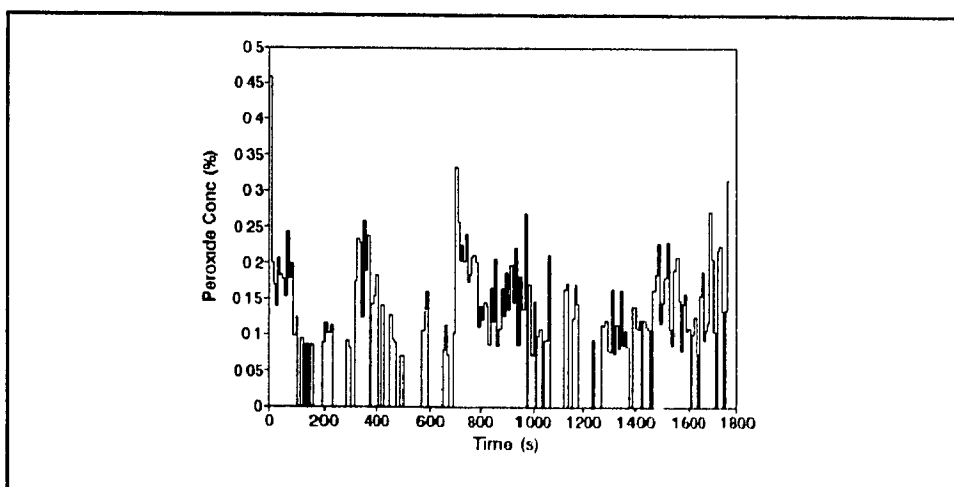


**Figure 6-9b:** Peroxide Concentration Data for Setpoint Tracking Experiment Using Internal Model Control

These results were obtained using a process model with a dead time  $t_d$  of 59 s, a process time constant  $\tau$  of 46 s, and a closed loop time constant  $\lambda_c$  of 180 s which was selected by trial and error. The control is very poor, indicating a severe problem with the process model.

Subsequent work made use of separate process models for positive and negative steps. The controller parameters used are shown in Table 6-4.

**Table 6-4: IMC Controller Tuning Parameters**

Controller Parameter	Setpoint Change	
	Positive	Negative
$K$ [kPa·s/% perox]	6.5	6.5
$t_d$ [s]	60	60
$\tau$ [s]	30	60
$\lambda_c$ [s]	60	60

Results for setpoint tracking using the above tuning parameters are shown in Figure 6-10.

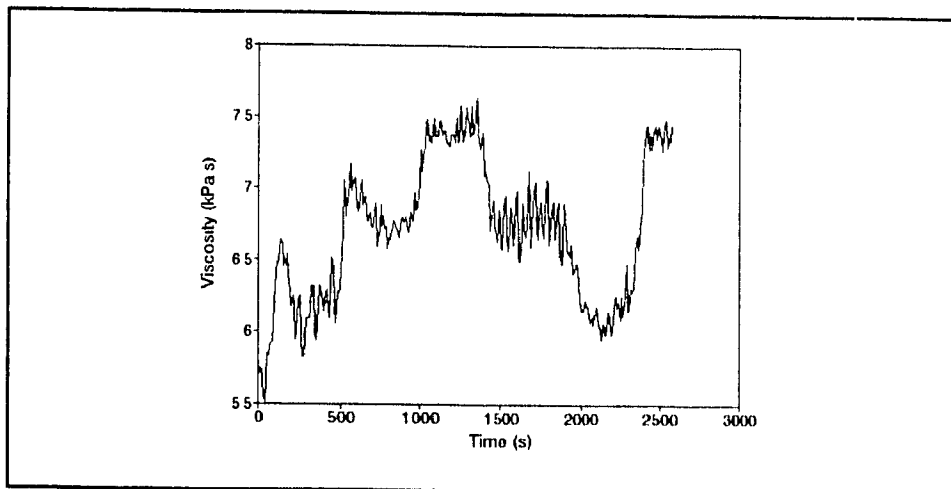


**Figure 6-10a:** Viscosity Data For Setpoint Tracking Experiment Using Internal Model Control

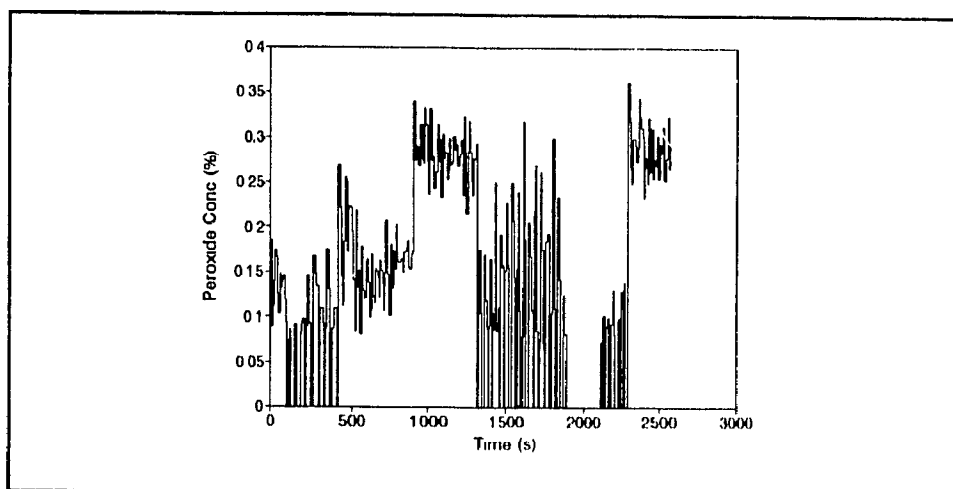


**Figure 6-10b:** Peroxide Concentration Data for Setpoint Tracking Experiment Using iMC

These results are for the MFI 1.05 dg/min material at a strain rate of  $5 \text{ s}^{-1}$ . Response times (defined as the difference in time from the setpoint change to the time when the qualitatively smoothed process output first reaches the new setpoint) for the 0.6 kPa·s setpoint changes range from 100 to 125 seconds, and the 1.2 kPa·s step exhibits a response time of 140 s. However, the overall control is poor, as is especially apparent over the time interval from 1300 to

2300 s, where the controller action is erratic. Note that values of 0 % peroxide concentration arise from both negative controller output as well as the gravimetric feeder's inability to meter flow rates of less than 1 kg/hr (0.0088 % peroxide concentration).

#### 6.4 Dahlin Controller Performance

The Dahlin control algorithm is a direct synthesis method in which the desired closed loop response of the process is specified to behave as follows:

$$\frac{\eta(z^{-1})}{C(z^{-1})} = \frac{\left(1 - e^{-\frac{T}{\lambda_c}}\right) z^{-\frac{\theta_c}{T}-1}}{1 - e^{-\frac{T}{\lambda_c}} z^{-1}} \quad (6-8)$$

For a FOPDT process model, the appropriate control equation is:

$$C_t(z^{-1}) = \frac{1 - e^{-\frac{T}{\lambda_c}}}{1 - e^{-\frac{T}{\lambda_c}} z^{-1} - \left(1 - e^{-\frac{T}{\lambda_c}}\right) z^{-\frac{\theta_c}{T}-1}} \frac{1 - \delta z^{-1}}{\omega} \eta_t \quad (6-9)$$

The process model given in Table 6-2 was used for the Dahlin control experiments. The sampling period  $T$  was 8 s; the closed loop deadtime  $\theta_c$  was chosen to be that of the open loop deadtime, 96 s, and the closed loop time constant  $\lambda_c$  was used as an adjustable parameter to tune the closed loop response.

Results for setpoint tracking experiments are shown in Figure 6-11.



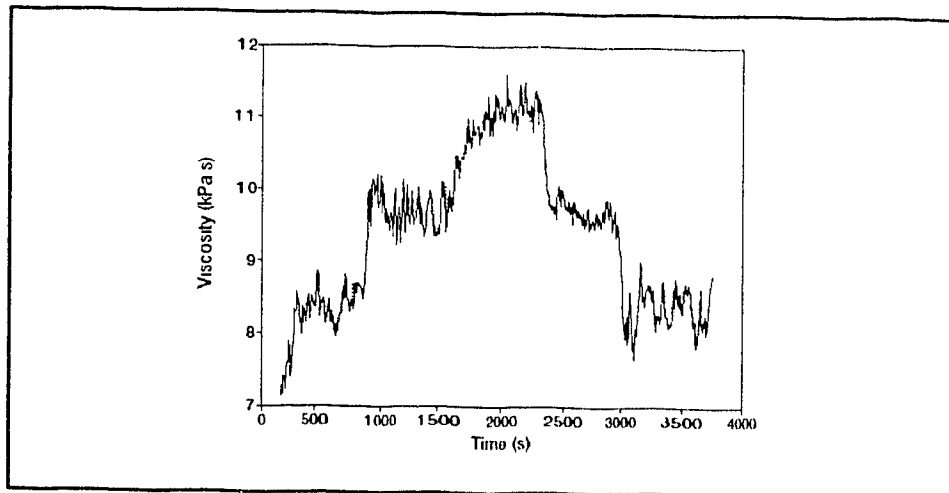


**Figure 6-11a:** Viscosity Data for Setpoint Tracking Experiment Using Dahlin's Algorithm

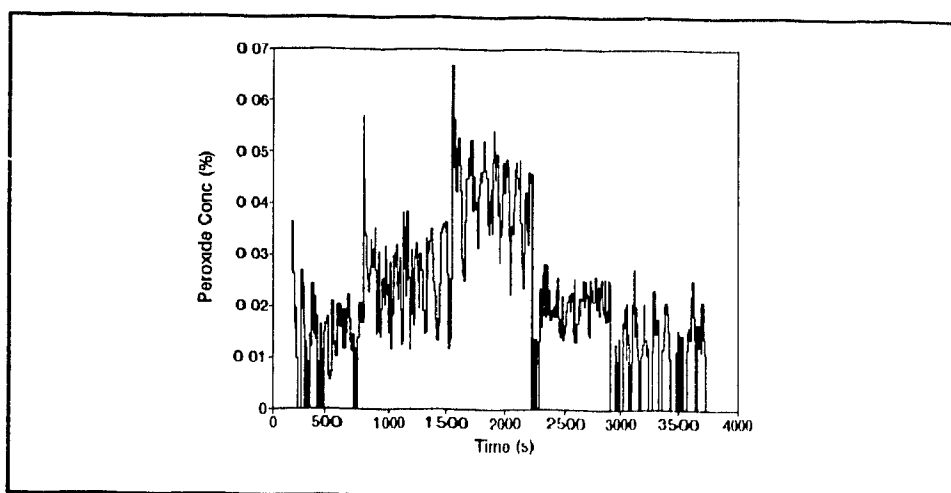


**Figure 6-11b.** Peroxide Concentration Data for Setpoint Tracking Experiment Using Dahlin's Algorithm

These results are for the MFI 1.05 dg/min material, with the dotted line in the upper graph representing 1.3 kPa·s steps in the viscosity setpoint. The value of the closed loop time constant  $\lambda_c$  was 24 s and was determined by trial and error. The response times range from 90 to 260 seconds. The data for the controlled variable, shown in the lower graph, demonstrate erratic controller action, an unfortunate result. Note that

values of 0 % peroxide concentration arise from the gravimetric feeder's inability to accurately meter flow rates of less than 1 kg/hr (0.088 % peroxide concentration) and are not the actual calculated outputs of the control algorithm.

Results for a load rejection experiment are shown in Figure 6-12.

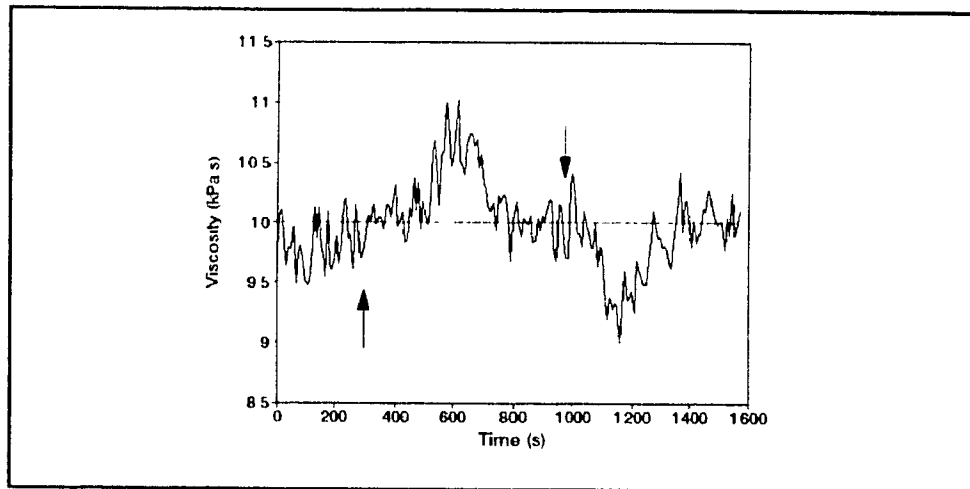


**Figure 6-12a:** Viscosity Data for Load Rejection Experiment Using Dahlin's Algorithm

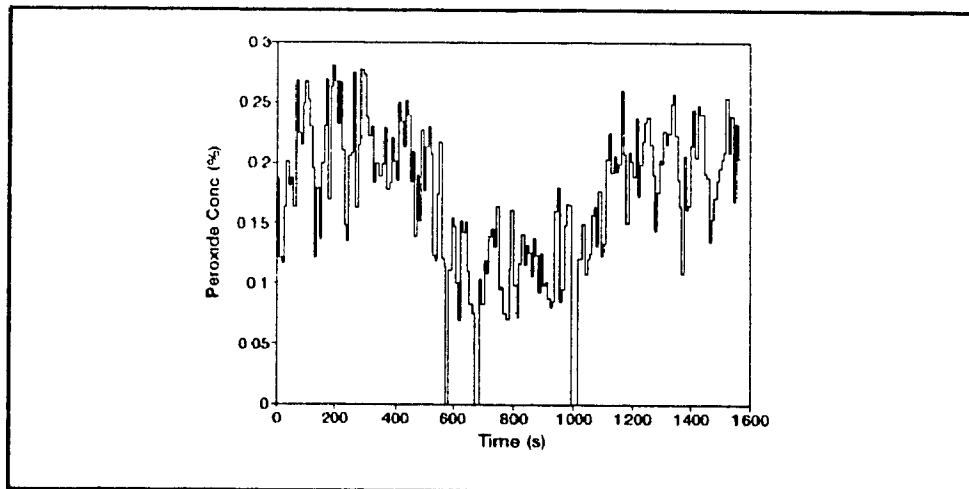


**Figure 6-11b** Perox Conc Data for Load Rejection Exper. Using Dahlin's Algorithm

The value of  $\lambda_c$  was 32 s. At the time indicated by the first arrow ( $\approx 300$  s) in the upper graph, the feed resin was changed

from MFI 1.05 to 0.56 dg/min, and the converse occurred at the time indicated by the second arrow ( $\approx 1000$  s). The controller successfully compensates for the load disturbances, achieving a response time of 430 and 290 s, respectively.

### 6.5 Minimum Variance Controller Performance

Nelson [7] successfully used minimum variance control techniques in order to compensate for the noise present in the viscosity measurement, which of course has an adverse effect on the controller performance. For the process model described in equation 6-4 with  $k = 3$ , the appropriate minimum variance control (MVC) equation is:

$$C_t(z^{-1}) = -\frac{1-\delta z^{-1}}{\omega} \frac{1-\theta}{1-\theta z^{-1}-(1-\theta)z^{-4}} \eta_t \quad (6-10)$$

Results of a setpoint tracking experiment using MVC is shown in Figure 6-13.

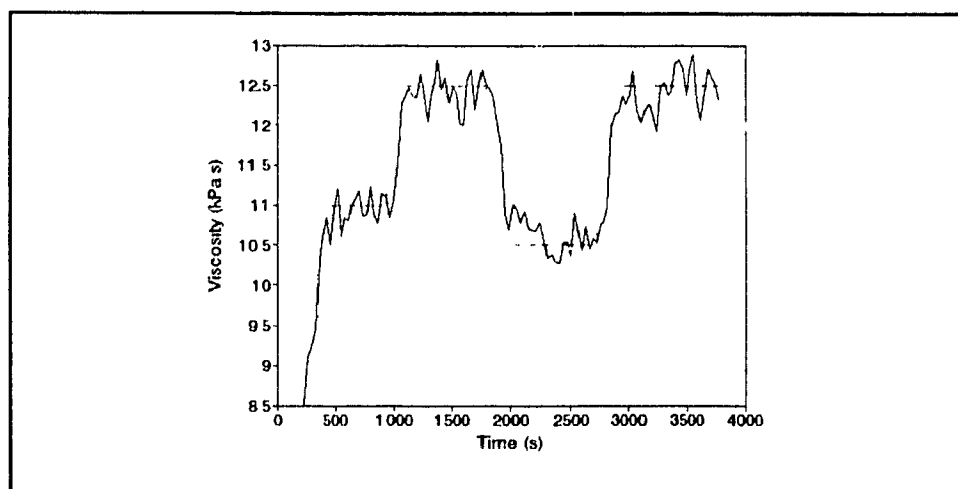


**Figure 6-13a:** Viscosity Data for Setpoint Tracking Experiment Using Minimum Variance Control

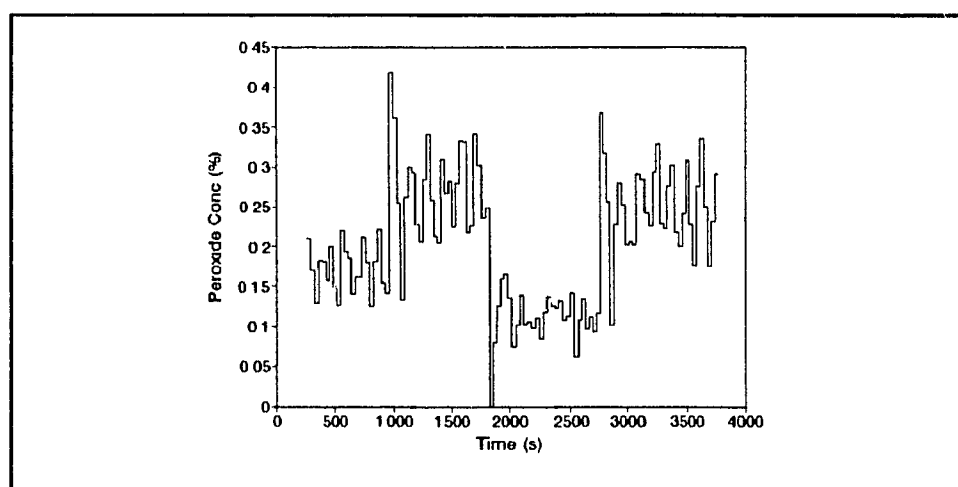


**Figure 6-13b:** Peroxide Concentration Data for Setpoint Tracking Experiment Using Minimum Variance Control

These results are for the MFI 0.56 dg/min material. The response times vary from 250 to 470 seconds for the 1.5-2 kPa·s steps in the viscosity setpoint. The control action, which is seen in the lower graph, is much less erratic than the previous results. This is quite encouraging from an industrial point of view, since the lifetime of the final control element is increased by reducing the amount of control

action performed, and longer response times are often willingly accepted for this reason in production environments. Unfortunately, this controller exhibited unsatisfactory load rejection performance during closed loop experimentation. The closed loop response to a load disturbance created by changing feed resins was undamped oscillation. Since the specific cause of this behaviour was not identified, this precludes any conclusions about the controller's suitability for the intended application.

#### 6.6 Summary

The closed loop experimental results are summarized in Table 6-5.

**Table 6-5: Summary of Closed Loop Control Results**

Controller	Response Time [s]	Control Quality	Manipulated Variable
IMC	100 - 140	noisy	much saturation
Dahlin	90 - 260	erratic	minimal saturation
MV	250 - 470	smooth	no saturation

IMC control experiments exhibited noisy control of viscosity and much saturation of the peroxide concentration at 0 %.

Dahlin control exhibited improved quality, although the

response was more erratic as response times varied from 90 to 260 s, almost a threefold increase. The manipulated variable did exhibit some saturation as well. MV control experiments exhibited smooth control, at the expense of longer response times, and no saturation of peroxide concentration occurred. However, successful load rejection experiments were only demonstrated with Dahlin control.

Controller performance was generally better at the higher viscosity setpoints. This can partially be attributed to gravimetric feeder performance, since the feeders operate erratically at flow rates of less than 2 kg/hr (0.018 % peroxide).

## **7. Accomplishments and Recommendations**

### **7.1 Summary of Accomplishments**

- 1) The problems posed by the effects of pressure and temperature on the rotating drum inline rheometer incorporating a disk-bar shear stress transducer were identified.
- 2) The performance of the SST temperature control loop was improved.
- 3) Both deterministic and stochastic first order plus deadtime models were identified for the response of recycled high density polyethylene viscosity to step changes in crosslinking agent concentration.
- 4) Closed loop control of HDPE crosslinking in a twin-screw extruder was demonstrated using the McGill ILR. Setpoint tracking was achieved using IMC, Dahlin, and minimum variance controllers. Load disturbance rejection was achieved with a Dahlin controller.

### **7.2 Recommendations**

#### **7.2.1 Gravimetric Feeders**

A significant factor in the mediocre closed loop

performance of the extruder and rheometer apparatus is attributed to the performance of the gravimetric feeders, as also experienced by Broadhead [4]. When closed loop control of HDPE crosslinking was first attempted, the feeder controller parameters that were used were those of Nelson [7], who achieved good closed loop performance, but in the present work these parameters were found to provide an underdamped response to setpoint changes. The underdamped response had a favorable effect on feeder response time but sometimes resulted in large overshoots in the response to setpoint changes and oscillations, leading to feeder controller error. Subsequently, the feeder controller parameters were adjusted by trial and error to provide an overdamped response, but this produced a new problem. The feeders became more sensitive to load disturbances, such as the refilling of the hopper with resin, and this made conducting long experiments with several setpoint changes difficult to achieve.

An improvement in the response of the remote gravimetric feeder (which feeds masterbatch) to load changes was made by replacement of the feeder screws used by Broadhead and Nelson with a different set. The original screws were of a hollow serpentine type and had an outside diameter roughly one half the inside diameter of the barrel. These were replaced with a set of solid Archimedean type screws that had a diameter close to that of the barrel. These screws are designed for use with powders but had a very beneficial effect on pellet feeding in



that the large surge that normally occurs when the hopper is filled (due to increased head) was reduced. Since only one set of these screws was available, the serpentine type screws were used in the overhead feeder. It is recommended, however, that for applications in which both feeders are used, a second set of Archimedean type screws (Control and Metering Ltd. TC-20-20) be installed in the overhead feeder.

Another possible remedy to the problem of feeder response would be to use a pump to inject the catalyst directly into the extruder barrel in liquid form, which would alleviate the need for the pellet feeder to also meter gravimetrically. A syringe pump would be best suited for this application. However, this method involves a potential safety hazard. The best mixing of catalyst with the resin would be achieved one of the last two sections of the extruder barrel where the screws are either entirely or almost entirely filled with polymer melt. Yet in order to feed in these sections, the catalyst injection port must contact the hot extruder barrel, potentially causing an organic peroxide type of catalyst to decompose within the feed line resulting in a fire or explosion. A proper installation would probably involve a water jacket surrounding the injection feed port with its own MACO 8000 temperature control loop.

During this study, the gravimetric feeders were interfaced to the MACO 8000, and any setpoint changes or output monitoring were performed by communicating with the

MACO. Broadhead and Nelson both recorded the feeder output by querying the MACO from the PC at frequent intervals. However, serial communications between the MACO and PC are somewhat unreliable. This problem worsened during this study until about three out four experiments failed due to serial communications errors. The serial communication algorithm was therefore modified to make it more robust, but this resulted in a three to fourfold increase in communication time. Querying the MACO for feeder data thus became less practical, and actual feeder output was not recorded. The tuning of the feeder microcontrollers was also done qualitatively since the feeder output was not recorded. This is an obvious drawback, especially since it is felt that the feeders are responsible for a great deal of the difficulty in controlling this process. It is recommended that the output of the gravimetric feeders be monitored directly by the PC. This will allow rapid sampling of the output, aiding quantitative feeder tuning techniques, and perhaps allowing implementation of closed loop control techniques where the feeders are modelled separately from the rest of the process.

#### **7.2.2 Large Pressure Drop in Rheometer**

Another problem was the restrictive nature of the rheometer channel and the resulting large pressure drop. The resins that Broadhead and Nelson used were substantially less viscous than the recycled HDPE used in the present study. The

use of the recycled HDPE thus resulted in a relatively large pressure drop through the rheometer. In order to prevent a high pressure in the rheometer, an exit die was not installed on the rheometer, and the flowrate was lowered to 8 kg/hr from the 12 kg/hr used in previous work. However, this further aggravated the feeder problem and worsened closed loop response. Should future work on high viscosity resins be performed, it is recommended that the exit area of the rheometer be remachined to be less restrictive.

### **7.2.3 Control of Strain Rate**

A final problem that was encountered in this work was the control of the strain rate at the lower end of the range around  $3 \text{ s}^{-1}$ . Since the servomotor features an internal control loop, the motor speed/input voltage relationship is very linear over the motor speed range as a whole, but there was often a consistent offset of about 6 % between motor setpoint and motor speed during an experiment. Since the strain rate appeared to deviate only by discrete values, which corresponded to a resolution of 11 bits over the speed range, it is believed that the resolution of the motor controller digital circuitry was incapable of adequately controlling the motor speed at the low end (84 rpm) of the motor speed range. It is recommended that for future work at lower strain rates, a gearbox that reduces the output speed even further be installed.

## References

- 1) Nelson, B.I., personal communication, May 1993.
- 2) Fritz, H.-G., Stöhrer, B., Intern. Polym. Proc., **1**, 31-41, 1986.
- 3) Pabedinskas, A., Cluett, W.R., Balke, S.T., Polym. Eng. Sci., **29**, 993-1003, 1989.
- 4) Broadhead, T.O., PhD Thesis, McGill University, Montreal, 1992.
- 5) Broadhead, T.O., Nelson, B.I., Dealy, J.M., Intern. Polym. Proc., **8**, 104-112, 1993.
- 6) Chen, T., M.Eng. Thesis, McGill University, Montreal, 1992.
- 7) Nelson, B.I., PhD Thesis, McGill University, Montreal, 1993.
- 8) Sentmanat, M.L., M.Eng. Thesis, McGill University, Montreal, 1992.
- 9) Nelson, B.I., **DTDRV Version 2.1 DT-2801-A Data Acquisition Routines, The MACODRV Version 2.1 PC-MACO 8000 Communications Program**, Dept. of Chem. Eng., McGill University, Montreal, 1990.
- 10) MATLAB, **MATLAB for MS-DOS Personal Computers**, The MathWorks, Inc., Natick, Mass., 1990.
- 11) Ljung, L., **System Identification Toolbox for Use With MATLAB**, The MathWorks, Inc., Natick, Mass., 1991.
- 12) Ljung, L., **System Identification: Theory for the User**, Prentice Hall, Englewood Cliffs, N.J., 1987.
- 13) Seborg, D.E., Edgar, T.F., Mellichamp, D.A., **Process Dynamics & Control**, John Wiley & Sons, New York, 1989.
- 14) Åström, K.J., Wittenmark, B., **Computer-Controlled Systems**, 2<sup>nd</sup> ed., Prentice Hall, Englewood Cliffs, N.J., 1990.
- 15) Bubic, F.R., **Process Rheometer - Model no: 3.45**, Dept. of Chem. Eng., McGill University, Montreal, 1988.

- 16) Dealy, J.M., Wissbrun, K.F., **Melt Rheology and its Role in Plastics Processing**, Van Nostrand Reinhold, New York, 1990.
- 17) Dealy, J.M., Broadhead, T.O., in: **Techniques in Rheological Measurement**, Collyer, Clegg, eds., Elsevier Applied Science, London, 1992.
- 18) Hamming, R.W., **Digital Filters**, 3<sup>rd</sup> ed., Prentice Hall, Englewood Cliffs, N.J., 1989.
- 19) Hertlein, T., Fritz, H.-G., SPE ANTEC Tech. Papers, 1593 1598, 1990.
- 20) MacGregor, J.F., **Optimal Stochastic Control Theory and Applications**, Dept. of Chem. Eng., McMaster University, Hamilton, Ont., 1982.
- 21) Smith, C.L., **Digital Computer Process Control**, Intext, Toronto, 1972.
- 22) Stephanopoulos, G., **Chemical Process Control: An Introduction to Theory and Practice**, Prentice Hall, Englewood Cliffs, N.J., 1984.
- 23) US Patent 4 463 928, 1984, Dealy, J.M.
- 24) US Patent 5 094 100, 1992, Dealy, J.M., Bubic, F.R., Doshi, S.R.

## A1. Appendix of Experimental Procedures

### A1.1 Typical Extruder Operating Conditions

A listing of the extruder and rheometer temperature setpoints are shown in Table A1-1.

**Table A1-1.** Typical Extruder Operating Temperature Setpoints

Temperature Control Zone	Temperature Setpoint [°C]
Extruder Zone 1	170
Extruder Zone 2	180
Extruder Zone 3	190
Extruder Zone 4	200
Rheometer Body	195
Rheometer Shaft	180
SST	180
Exit Die	190

A list of other extruder operating setpoints is shown in Table A1-2.

**Table A1-2: Typical Extrusion Parameter Setpoints**

69

Extrusion Parameter	Setpoint
Screw Speed [rpm]	300
Vacuum [kPa]	-90
Throughput [kg/hr]	8

### **A1.2 Preparation of Masterbatch**

The masterbatch consisted of the same recycled resin used for the feed, with a 0.07 % concentration of Lupersol 101 liquid peroxide (Atochem) and also a 0.28 % concentration of light paraffin oil which was used to help disperse the peroxide. The first step was to dilute the peroxide to a concentration of 20 % in the paraffin oil. Then, this mixture was poured over the HDPE pellets in a high shear mixer and was mixed for 5 minutes in order to obtain a concentration of 0.07 % peroxide.

### **A1.3 Experimental Procedure**

- 1) Turn on extruder and rheometer heating system. Turn on external power supply, motor controller, and temperature indicator. Open cooling water valve.
- 2) Wait until system has reached temperature setpoints.
- 3) Fill up feeder hoppers with resin and masterbatch.

- 4) Install smallest exit die on rheometer. Remove plug on the SST purge tube.
- 5) Run the extruder on resin until the purge stream appears to composed of fresh material. Replace plug and let extruder run for several more minutes.
- 6) Stop extruder. Remove exit die. Run the extruder on resin.
- 7) Turn on the rheometer motor by means of the PC.
- 8) Wait until the rheometer and gap temperatures reach steady state.
- 9) Using PC control: Turn off the rheometer motor. Wait 5 seconds. Record the SST baseline voltage. Turn on rheometer motor.
- 10) Execute remainder of control program on PC. This will vary depending on whether system identification or closed loop control is the objective of the experiment. Fill up hoppers as required.
- 11) Turn off extruder. Turn off external power supply, motor controller, and temperature indicator. Close cooling water valve.



## A2. Appendix of Software Listings

### A2.1 PRBS System Identification Experiment Program

```

DECLARE SUB PRBSGEN (PRBS%(), NS%, NP%)
DECLARE SUB BW3OLP (RAWDAT%(), RESULT'())
DECLARE SUB PLOTGRPH (VISCDAT'(), NUMDAT%)

'$INCLUDE 'MACODEC.BAS'
'$INCLUDE 'DT2-1DEC.BAS'
'$DYNAMIC
'-----

'Feb 15, 1993 Tony Pillo
'-----

CONST CWSTRAIN = 3 35, GAPHEAT = 5, NREP = 1 5
DTFREQ' = 500

DIM RAWDATA%(4, 199), FILTDAT'(4)

MACO INIT 1, 1, -1
DT.INIT
DT CLOCK DTFREQ'
DT SETADC 1, 0, 4, 1000
DT DPSET 0, 1, 0
'-----

CLS
SCREEN 13
COLOR 14
LOCATE 1, 12
PRINT "McGILL ILR"
LOCATE 2, 11
PRINT "PRBS PROGRAM"
COLOR 2
LOCATE 4, 1
INPUT "Total feed rate (kg/hr)"; TOTFEED'
LOCATE 6, 1
INPUT "Mb step feed rate (kg/hr)", STEPFEED'
LOCATE 8, 1
INPUT "Number of PRBS stages ", NS%
LOCATE 10, 1
INPUT "Number of samp per / step ", NP%
LOCATE 12, 1
INPUT "Data filename", NAME$

CLS
NSTEP% = INT(NP% * (2 ^ NS% - 1) + .5)
NTOT% = INT(NSTEP% * NREP / NP%) * NP%
DIM PRBS%(NSTEP% - 1), VISCDATA'(7, NTOT% - 1)
PRBSGEN PRBS%(), NS%, NP%
LOCATE 24, 1
COLOR 14
INPUT "Press {Enter} to continue", DUMMY$
COLOR 2

CLS
SCREEN 12
LOCATE 17, 2
PRINT "Time (s)"
LOCATE 17, 12
PRINT "Viscosity (kPa s)"
COLOR 7
VIEW PRINT 18 TO 27
'-----

REMOTFDR2% = STEPFEED' * 100
OVERFDR1% = TOTFEED' * 100

```

```

OVERFDP2% = (TOTFEED! - STEPFEED!) * 100

DT DAOUT 0, GAPHEAT * 6 7396 + 2046 2
DT DPW 0, 1, 1

INPUT "Press {Enter} to get baseline ", DUMMY$

DT.DPW 0, 1, 0
TIME' = TIMER + 5
DO UNTIL ABS(TIME' - TIMER) < 1
LOOP

DT MLTADC RAWDATA%()
BW30LP RAWDATA%(), FILTDAT'()
BASELINE' = FILTDAT'(3)

DT DAOUT 0, CWSTRAIN * 6 7396 + 2046 2
DT DPW 0, 1, 1
TIME' = TIMER + 1
DO UNTIL ABS(TIME' - TIMER) < 1
LOOP

INIT TIME! = TIMER
FOR DATACOUNT% = 0 TO NTOT% - 1

  IF DATACOUNT% > NSTEP% - 1 THEN
    INDEX% = DATACOUNT% - NSTEP%
  ELSE
    INDEX% = DATACOUNT%
  END IF

  DO UNTIL (INT((TIMER - INIT TIME') * 10) MOD 320) = 0
  LOOP
  IF DATACOUNT% = 0 THEN
    IF PRBS%(INDEX%) = 0 THEN
      DO
        MACO OPEN
        MACO SET "DRS2", OVERFDR1%, MERR%
        MACO CLOSE
        LOOP UNTIL MERR% = 0
      DO
        MACO OPEN
        MACO.W OPCR 2705, 0, MERR%
        MACO CLOSE
        LOOP UNTIL MERR% = 0
      ELSE
        DO
          MACO.OPEN
          MACO.SET "DRS2", OVERFDR2%, MERR%
          MACO.CLOSE
          LOOP UNTIL MERR% = 0
        DO
          MACO OPEN
          MACO.SET "DRS3", REMOTFDR2%, MERR%
          MACO CLOSE
          LOOP UNTIL MERR% = 0
        DO
          MACO OPEN
          MACO.W OPCR 2705, 1, MERR%
          MACO CLOSE
          LOOP UNTIL MERR% = 0
        END IF
      ELSEIF PRBS%(INDEX%) <> LASTINDEX% THEN
        IF PRBS%(INDEX%) = 0 THEN
          DO
            MACO OPEN
            MACO.SET "DRS2", OVERFDR1%, MERR%
            MACO.CLOSE
            LOOP UNTIL MERR% = 0
          DO
            MACO.OPEN
            MACO.W OPCR 2705, 0, MERR%
            MACO CLOSE
            LOOP UNTIL MERR% = 0
          ELSE
            DO
              MACO OPEN
              MACO SET "DRS2", OVERFDR2%, MERR%

```

```

MACO.CLOSE
LOOP UNTIL MERR% = 0
DO
    MACO.OPEN
    MACO.SET "DRS3", REMOTFDR2%, MERR%
    MACO.CLOSE
    LOOP UNTIL MERR% = 0
    DO
        MACO.OPEN
        MACO.W.OPCR 2705, 1, MERR%
        MACO.CLOSE
        LOOP UNTIL MERR% = 0
    END IF
END IF

DT.MLTADC RAWDATA%()

VISCDATA!(0, DATACOUNT%) = TIMER - INIT TIME!
BW3OLP RAWDATA%(), FILTDAT!()

VISCDATA!(2, DATACOUNT%) = FILTDAT!(0) * 23.073 + 005968
VISCDATA!(3, DATACOUNT%) = FILTDAT!(1) * 637 - 434
VISCDATA!(4, DATACOUNT%) = FILTDAT!(2) * 629 - 338
VISCDATA!(5, DATACOUNT%) = FILTDAT!(3)
VISCDATA!(6, DATACOUNT%) = FILTDAT!(4) * 3 + 170
VISCDATA!(7, DATACOUNT%) = PRBS%(INDEX%)
MEAS' = VISCDATA!(5, DATACOUNT%)
TEMP' = VISCDATA!(6, DATACOUNT%)
TACH' = VISCDATA!(2, DATACOUNT%)

IF TEMP' < 185.8 THEN
    SSTCAL' = (8 10238 - 8 53151) / (185.8 - 181.5) * (TEMP' - 181.5) + 8 53151
ELSEIF (TEMP' >= 185.8) AND (TEMP' <= 191.1) THEN
    SSTCAL' = (8 01556 - 8 10238) / (191.1 - 185.8) * (TEMP' - 185.8) + 8 10238
ELSEIF TEMP' > 191.1 THEN
    SSTCAL' = (7 65671 - 8.01556) / (196.1 - 191.1) * (TEMP' - 191.1) + 8 01556
END IF

VISC' = (MEAS' - BASELINE') / (TACH' * EXP(1595.3 * (1 / (TEMP' + 273.15) - 1 / 463.15)))
* SSTCAL!
VISCDATA!(1, DATACOUNT%) = VISC'

COLOR 3
PRINT USING "    ###.## ", VISCDATA!(0, DATACOUNT%),
PRINT USING "    ###.### ", VISCDATA!(1, DATACOUNT%),
PRINT USING "    #   ", VISCDATA!(2, DATACOUNT%)
IF DATACOUNT% > 1 THEN
    PLOTGRPH VISCDATA!(), DATACOUNT%
END IF

LASTINDEX% = PRBS%(INDEX%)

NEXT DATACOUNT%

DT.DPW 0, 1, 0

OPEN "O", 1, ".\APR\" + NAME$
FOR COUNT5% = 0 TO NTOT% - 1
    PRINT #1, VISCDATA!(0, COUNT5%);
    PRINT #1, VISCDATA!(1, COUNT5%);
    PRINT #1, VISCDATA!(2, COUNT5%);
    PRINT #1, VISCDATA!(3, COUNT5%);
    PRINT #1, VISCDATA!(4, COUNT5%);
    PRINT #1, VISCDATA!(5, COUNT5%);
    PRINT #1, VISCDATA!(6, COUNT5%);
    PRINT #1, VISCDATA!(7, COUNT5%)
NEXT COUNT5%
CLOSE

OPEN "O", 1, " \APR\" + NAME$ + " DAT"
FOR COUNT6% = (NTOT% - NSTEP%) TO NTOT% - 1
    PRINT #1, VISCDATA!(1, COUNT6%);
    PRINT #1, VISCDATA!(7, COUNT6%)
NEXT COUNT6%
CLOSE

END

```

```

REM $STATIC
SUB BW3OLP (RAWDAT%, RESULT%)
,
DIM X N 3'(4), X N 2'(4), X N 1'(4), X N'(4)
DIM Y N 3'(4), Y N 2'(4), Y N 1'(4), Y N'(4)
DIM DATUM'(4, 199)
,
FOR DC% = 0 TO 199
  FOR C1% = 0 TO 4
    X N'(C1%) = RAWDAT%(C1%, DC%) / 204.8 - 10
    IF DC% > 0 THEN
      X N.1'(C1%) = RAWDAT%(C1%, DC% - 1) / 204.8 - 10
      Y N 1'(C1%) = DATUM'(C1%, DC% - 1)
    END IF
    IF DC% > 1 THEN
      X N 2'(C1%) = RAWDAT%(C1%, DC% - 2) / 204.8 - 10
      Y N 2'(C1%) = DATUM'(C1%, DC% - 2)
    END IF
    IF DC% > 2 THEN
      X N 3'(C1%) = RAWDAT%(C1%, DC% - 3) / 204.8 - 10
      Y N 3'(C1%) = DATUM'(C1%, DC% - 3)
    END IF
    Y N'(C1%) = 00041654613908# * X N'(C1%) + .00124963841723# * X N.1'(C1%) +
    00124963841723# * X N 2'(C1%) + 00041654613908# * X N 3'(C1%)
    Y N'(C1%) = Y N'(C1%) + 2.68615739654814# * Y N.1'(C1%) - 2.41965511096647# *
    Y N 2'(C1%) + 73016534530572# * Y N 3'(C1%)
    DATUM'(C1%, DC%) = Y N'(C1%)
  NEXT C1%
NEXT DC%
,
FOR C2% = 0 TO 4
  SUM' = 0
  FOR C3% = 100 TO 199
    SUM' = SUM' + DATUM'(C2%, C3%)
  NEXT C3%
  RESULT'(C2%) = SUM' / 100
NEXT C2%
,
END SUB

SUB PLOTGRPH (VISCDAT%, NUMDAT%)
,
VIEW (200, 0)-(639, 240)
CLS
,
X MIN' = VISCDAT%(0, 0)
X MAX' = VISCDAT%(0, NUMDAT%)
Y MIN' = VISCDAT%(1, 0)
Y MAX' = VISCDAT%(1, 0)
FOR SORT% = 1 TO NUMDAT%
  IF VISCDAT%(1, SORT%) > Y MAX' THEN
    Y MAX' = VISCDAT%(1, SORT%)
  ELSEIF VISCDAT%(1, SORT%) < Y MIN' THEN
    Y MIN' = VISCDAT%(1, SORT%)
  END IF
NEXT SORT%
,
WINDOW (X MIN', Y MIN')-(X MAX', Y MAX')
COLOR 15
LINE (X MIN', Y MIN')-(X MIN', Y MAX')
LINE (X MIN', Y MIN')-(X MAX', Y MIN')
COLOR 2
FOR PLOT% = 1 TO NUMDAT%
  LINE (VISCDAT%(0, PLOT% - 1), VISCDAT%(1, PLOT% - 1))-(VISCDAT%(0, PLOT%), VISCDAT%(1,
  PLOT%))
NEXT PLOT%
,
END SUB

SUB PRBSGEN (PRBS%(), NS%, NP%)
,
PRINT
INPUT "Number of feedback stages ", NP%
N% = INT(2 ^ NS% - 1 + 5)
DIM R%(NS%), FBS%(NP%), W%(N%)
FOR I% = 1 TO NP%
  PRINT
  PRINT "Stage #", I%, " ",

```

```

INPUT "", FBS%(I%)
IF FBS%(I%) < 1 OR FBS%(I%) > NS% THEN PRINT "Error, stage no good" STOP
NEXT I%
PRINT
FOR I% = 1 TO NS%
  R%(I%) = 1
NEXT I%
FOR I% = 1 TO N%
  S% = 0
  FOR J% = 1 TO NF%
    S% = S% + R%(FBS%(J%))
  NEXT J%
  S% = S% MOD 2
  PRINT R%(NS%),
  W%(I%) = R%(NS%)
  FOR J% = NS% TO 2 STEP -1
    R%(J%) = R%(J% - 1)
  NEXT J%
  R%(1) = S%
NEXT I%
PRINT
FOR I% = 0 TO N% - 1
  FOR J% = 0 TO NP% - 1
    PRBS%(I% * NP% + J%) = W%(I% + 1)
  NEXT J%
NEXT I%
END SUB

```

## A2.2 Minimum Variance Control Program

```

DECLARE SUB BW3OLP (RAWDAT%(), RESULT'())
DECLARE SUB PLOTGRPH (VISCDAT'(), NUMDAT%)

'$INCLUDE 'MACODEC.BAS'
'$INCLUDE 'DT2-1DEC.BAS'
'$DYNAMIC

'-----
'Mar. 17, 1993 Tony Pillo.
'-----

CONST MASSFLOW = 8, TOTFLOW% = MASSFLOW * 100, CWSTRAIN = 3.35, GAPHEAT = 5,
DTFREQ! = 500

DIM VISCDATA!(8, 1999), RAWDATA%(4, 199), FILTDAT'(4)

MACO.INIT 1, 1, -1
DT INIT
DT.CLOCK DTFREQ!
DT.SETADC 1, 0, 4, 1000
DT.DPSET 0, 1, 0

'-----

CLS
SCREEN 13
COLOR 14
LOCATE 1, 12
PRINT "MCGILL RDIR"
LOCATE 2, 1
PRINT "Minimum Variance Control"
COLOR 2
LOCATE 4, 1
INPUT "Data filename"; NAME$
CLS
SCREEN :2
COLOR 12
LOCATE 2, 9

```

```

PRINT "McGILL RDIR"
LOCATE 4, 1
PRINT "Minimum Variance Control"
COLOR 14
LOCATE 17, 2
PRINT "Time (s)"
LOCATE 17, 12
PRINT "Viscosity (kPa s)"
COLOR 5
LOCATE 27, 1 PRINT "F1",
LOCATE 27, 19 PRINT "F2",
LOCATE 27, 37 PRINT "F3",
LOCATE 28, 1 PRINT "F4",
LOCATE 28, 19 PRINT "F5",
LOCATE 28, 37 PRINT "F6",
COLOR 6
LOCATE 27, 4 PRINT "Close Loop",
LOCATE 27, 22 PRINT "St Pt Change",
LOCATE 27, 40 PRINT "2nd St Pt",
LOCATE 28, 4 PRINT "3rd St Pt",
LOCATE 28, 22 PRINT "4th St Pt",
LOCATE 28, 40 PRINT "5th St Pt",
COLOR 7
VIEW PRINT 18 TO 26

```

```

-----
DT DAOUT 0, GAPHEAT * 6.7396 + 2046.2
DT DPW 0, 1, 1

INPUT "Press {Enter} to get baseline ", DUMMY$

DT DPW 0, 1, 0
TIME! = TIMER + 5
DO UNTIL ABS(TIME! - TIMER) < .1
LOOP

DT MLTADC RAWDATA%()
BW3OLP RAWDATA%(), FILTDAT%()
BASELINE! = FILTDAT%(3)

DT DAOUT 0, CWSTRAIN * 6.7396 + 2046.2
DT DPW 0, 1, 1
TIME! = TIMER + 1
DO UNTIL ABS(TIME! - TIMER) < 1
LOOP

INIT TIME! = TIMER
DATACOUNT% = 0
WHILE KEY$ <> CHR$(27)

DO UNTIL (INT((TIMER - INIT.TIME!) * 10) MOD 320) = 0
LOOP
DT.MLTADC RAWDATA%()

VISCDATA%(0, DATACOUNT%) = TIMER - INIT.TIME!
OLD TIME! = MEAS TIME!
MEAS TIME! = VISCDATA%(0, DATACOUNT%)
BW3OLP RAWDATA%(), FILTDAT%()

VISCDATA%(4, DATACOUNT%) = FILTDAT%(0) * 23.073 + .005968
VISCDATA%(5, DATACOUNT%) = FILTDAT%(1) * 637 - 434
VISCDATA%(6, DATACOUNT%) = FILTDAT%(2) * 629 - 338
VISCDATA%(7, DATACOUNT%) = FILTDAT%(3)
VISCDATA%(8, DATACOUNT%) = FILTDAT%(4) * 3 + 170
MEAS! = VISCDATA%(7, DATACOUNT%)
TEMP! = VISCDATA%(8, DATACOUNT%)
TACH! = VISCDATA%(4, DATACOUNT%)

IF TEMP! < 185.8 THEN
SSTCAL! = (8.10238 - 8.53151) / (185.8 - 181.5) * (TEMP! - 181.5) + 8.53151
ELSEIF (TEMP! >= 185.8) AND (TEMP! <= 191.1) THEN
SSTCAL! = (8.01556 - 8.10238) / (191.1 - 185.8) * (TEMP! - 185.8) + 8.10238
ELSEIF TEMP! > 191.1 THEN
SSTCAL! = (7.65671 - 8.01556) / (196! - 191.1) * (TEMP! - 191.1) + 8.01556
END IF

U N 4! = U N 3! U N 3! = U N 2! U N 2! = U N 1!: U N 1! = U N!

```

```

Y.N.1' = Y.N' * X.N.1' = X.N'

Y N' = (MEAS' - BASELINE') / (TACH' * EXP(1595.3 * (1 / (TEMP' + 273.15) - 1 / 461.15))) *
SSTCAL!
VISCDATA!(1, DATACOUNT%) = Y N'

IF KEY$ = CHR$(0) + CHR$(59) THEN
  COLOR 5 PRINT
  INPUT "New Setpoint", X N'
  X N.1' = Y.N.1'
  COLOR 2
  CONTROLON% = -1
ELSEIF KEY$ = CHR$(0) + CHR$(60) THEN
  COLOR 5 PRINT
  INPUT "New Setpoint", X.N'
  COLOR 2
ELSEIF KEY$ = CHR$(0) + CHR$(61) THEN
  COLOR 5 PRINT
  INPUT "New Setpoint", X.N'
  COLOR 2
ELSEIF KEY$ = CHR$(0) + CHR$(62) THEN
  COLOR 5 PRINT
  INPUT "New Setpoint", X N'
  COLOR 2
ELSEIF KEY$ = CHR$(0) + CHR$(63) THEN
  COLOR 5 PRINT
  INPUT "New Setpoint", X.N'
  COLOR 2
ELSEIF KEY$ = CHR$(0) + CHR$(64) THEN
  COLOR 5 PRINT
  INPUT "New Setpoint", X.N'
  COLOR 2
END IF
VISCDATA!(2, DATACOUNT%) = X N'

E.N.1' = Y.N.1' - X.N.1' E.N' = Y N' - X N'

```

```

IF CONTROLON% THEN
  U.N' = 506209 * U.N.1' + .493791 * U.N.4' - 1.60451 * E.N' + 1.08528 * E.N.1'
  OLDFDR1% = OVERFDR%
  OLDFDR2% = REMOTFDR%
  OVERFDR% = (MASSFLOW - U.N') * 100
  REMOTFDR% = U.N' * 100
  IF (REMOTFDR% > TOTFLOW%) OR (OVERFDR% < 50) THEN
    REMOTFDR% = TOTFLOW%
  END IF
  IF (OVERFDR% > TOTFLOW%) OR (REMOTFDR% < 50) THEN
    OVERFDR% = TOTFLOW%
  END IF
  IF REMOTFDR% > 50 THEN
    DO
      MACO.OPEN
      MACO.SET "DRS3", REMOTFDR%, MERR%
      MACO.CLOSE
      LOOP UNTIL MERR% = 0
    ELSE
      DO
        MACO.OPEN
        MACO.W.OPCR 2705, 0, MERR%
        MACO.CLOSE
        LOOP UNTIL MERR% = 0
      END IF
    IF OVERFDR% > 50 THEN
      DO
        MACO.OPEN
        MACO.SET "DRS2", OVERFDR%, MERR%
        MACO.CLOSE
        LOOP UNTIL MERR% = 0
      ELSE
        DO
          MACO.OPEN
          MACO.W.OPCR 2704, 0, MERR%
          MACO.CLOSE
          LOOP UNTIL MERR% = 0
        END IF
      IF (OLDFDR2% <= 50) AND (REMOTFDR% > 50) THEN

```

```

DO
  MACO.OPEN
  MACO W OPCR 2705, 1, MERR%
  MACO CLOSE
  LOOP UNTIL MERR% = 0
END IF
IF (OLDFDP1% <= 50) AND (OVERFDR% > 50) THEN
  DO
    MACO.OPEN
    MACO W OPCR 2704, 1, MERR%
    MACO CLOSE
    LOOP UNTIL MERR% = 0
  END IF
END IF
VISCDATA!(3, DATACOUNT%) = U N'

-----

COLOR 3
PRINT USING "    ### ## ", VISCDATA!(0, DATACOUNT%);
PRINT USING "    ###.### ", VISCDATA!(1, DATACOUNT%);
PRINT USING "    # ##", VISCDATA!(4, DATACOUNT%)
IF DATACOUNT% > 2 THEN
  PLOTGRPH VISCDATA!(), DATACOUNT%
END IF

KEY$ = INKEY$
DATACOUNT% = DATACOUNT% + 1

WEND

DT DPW 0, 1, 0

OPEN "O", 1, " \APR\" + NAME$

FOR COUNT5% = 0 TO DATACOUNT% - 1
  PRINT #1, VISCDATA!(0, COUNT5%);
  PRINT #1, VISCDATA!(1, COUNT5%);
  PRINT #1, VISCDATA!(2, COUNT5%);
  PRINT #1, VISCDATA!(3, COUNT5%);
  PRINT #1, VISCDATA!(4, COUNT5%);
  PRINT #1, VISCDATA!(5, COUNT5%);
  PRINT #1, VISCDATA!(6, COUNT5%);
  PRINT #1, VISCDATA!(7, COUNT5%);
  PRINT #1, VISCDATA!(8, COUNT5%)
NEXT COUNT5%

CLOSE

END

REM $STATIC
SUB BW3OLP (RAWDAT%(), RESULT%())
,
DIM X N 3'(4), X N 2'(4), X.N 1'(4), X.N'(4)
DIM Y N 3'(4), Y N 2'(4), Y.N 1'(4), Y.N'(4)
DIM DATUM'(4, 199)
,
FOR DC% = 0 TO 199
  FOR C1% = 0 TO 4
    X N'(C1%) = RAWDAT%(C1%, DC%) / 204.8 - 10
    IF DC% > 0 THEN
      X N.1'(C1%) = RAWDAT%(C1%, DC% - 1) / 204.8 - 10
      Y N 1'(C1%) = DATUM'(C1%, DC% - 1)
    END IF
    IF DC% > 1 THEN
      X N 2'(C1%) = RAWDAT%(C1%, DC% - 2) / 204.8 - 10
      Y N 2'(C1%) = DATUM'(C1%, DC% - 2)
    END IF
    IF DC% > 2 THEN
      X N 3'(C1%) = RAWDAT%(C1%, DC% - 3) / 204.8 - 10
      Y N 3'(C1%) = DATUM'(C1%, DC% - 3)
    END IF
    Y N#(C1%) = 00041654613908# * X N'(C1%) + 00124963841723# * X N.1'(C1%) +
    00124963841723# * X N 2'(C1%) + 00041654613908# * X.N.3'(C1%)
    Y N#(C1%) = Y N#(C1%) + 2.68615739654814# * Y.N.1'(C1%) - 2.41965511096647# *
    Y N 2'(C1%) + 73016534530572# * Y N 3'(C1%)
    DATUM'(C1%, DC%) = Y.N#(C1%)
  
```



```

      NEXT C1%
NEXT DC%
,
FOR C2% = 0 TO 4
  SUM' = 0
  FOR C3% = 100 TO 199
    SUM' = SUM' + DATUM'(C2%, C3')
  NEXT C3%
  RESULT'(C2%) = SUM' / 100
NEXT C2%
,
END SUB

SUB PLOTGRPH (VISCDAT'(), NUMDAT%)
,
VIEW (200, 0)-(639, 240)
CLS
,
X.MIN' = VISCDAT'(0, 0)
X.MAX' = VISCDAT'(0, NUMDAT%)
Y.MIN' = VISCDAT'(1, 0)
Y.MAX' = VISCDAT'(1, 0)
FOR SORT% = 1 TO NUMDAT%
  IF VISCDAT'(1, SORT%) > Y.MAX' THEN
    Y.MAX' = VISCDAT'(1, SORT%)
  ELSEIF VISCDAT'(1, SORT%) < Y.MIN' THEN
    Y.MIN' = VISCDAT'(1, SORT%)
  END IF
NEXT SORT%
,
WINDOW (X.MIN', Y.MIN')-(X.MAX', Y.MAX')
COLOR 15
LINE (X.MIN', Y.MIN')-(X.MIN', Y.MAX')
LINE (X.MIN', Y.MIN')-(X.MAX', Y.MIN')
COLOR 2
FOR PLOT% = 1 TO NUMDAT%
  LINE (VISCDAT'(0, PLOT% - 1), VISCDAT'(1, PLOT% - 1))-(VISCDAT'(0, PLOT%), VISCDAT'(1,
PLOT%))
NEXT PLOT%
,
END SUB

```

### A3. Appendix of Equipment Drawings

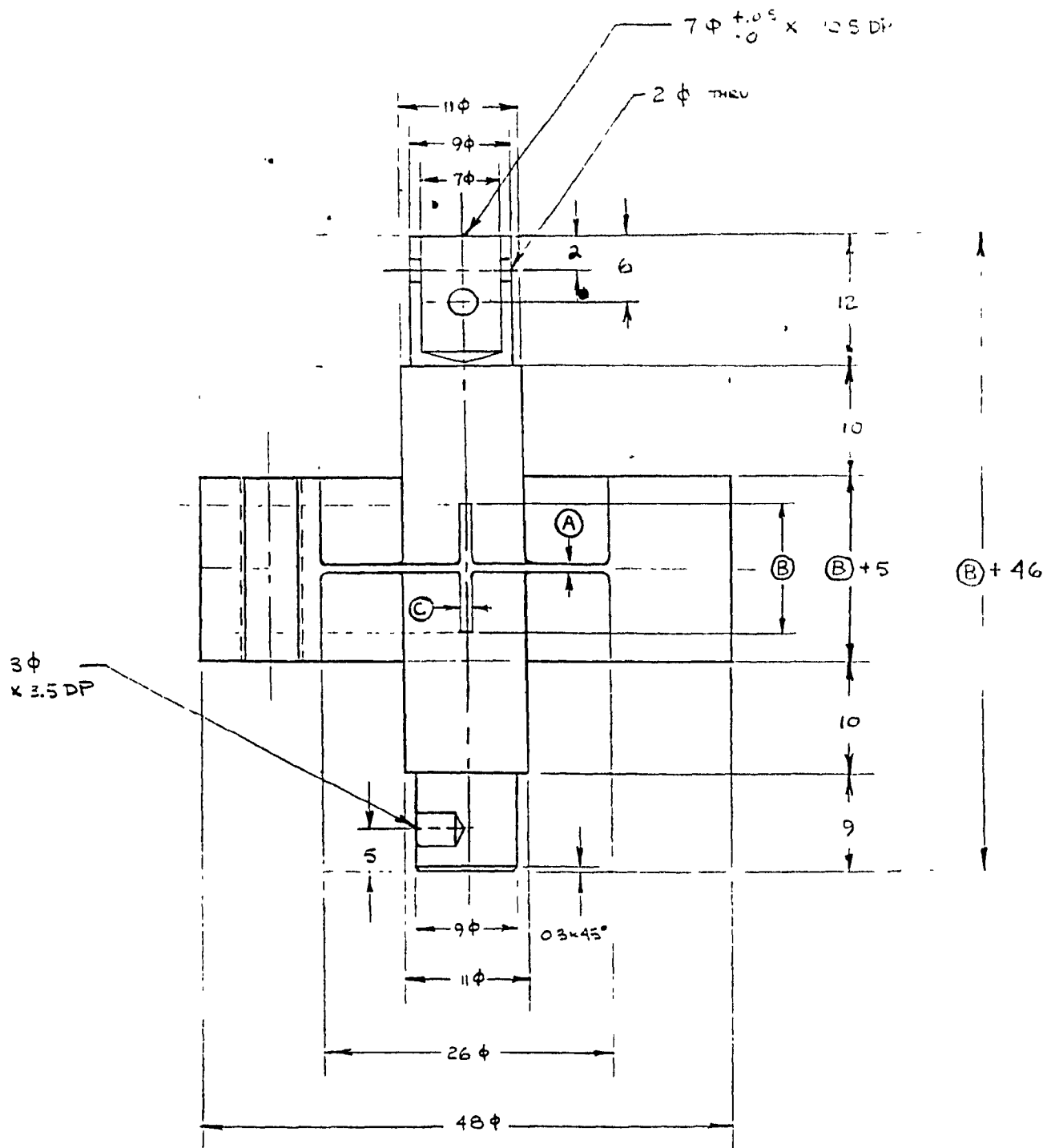
#### A3.1 Shear Stress Transducer CAD Analysis

##### Transducer Data

---

Maximum measured shear stress:	(MPa)	.08
Minimum measured shear stress:	(MPa)	.00016
Maximum bending stress in bar:	(MPa)	8.050078
Maximum shear stress in bar:	(MPa)	12.81369
Maximum melt pressure:	(MPa)	3.5
Maximum axial deflection:	(mm)	.00005
Maximum deflection at probe:	(mm)	.0254
Minimum deflection at probe:	(mm)	.0000508
Maximum active face deflection:	(mm)	1.063256E-02
Minimum active face deflection:	(mm)	2.126512E-05
Active face diameter:	(mm)	8
Disk outside diameter:	(mm)	26
Disk inside diameter:	(mm)	11
Disk thickness:	(mm)	.6380798
Torsion bar cross-sectional height:	(mm)	17.01721
Torsion bar cross-sectional width:	(mm)	1.063576
Lever lengths - Active face end	(mm)	36
Probe end	(mm)	86

## A3.2 Shear Stress Transducer, Disk-Bar Detail



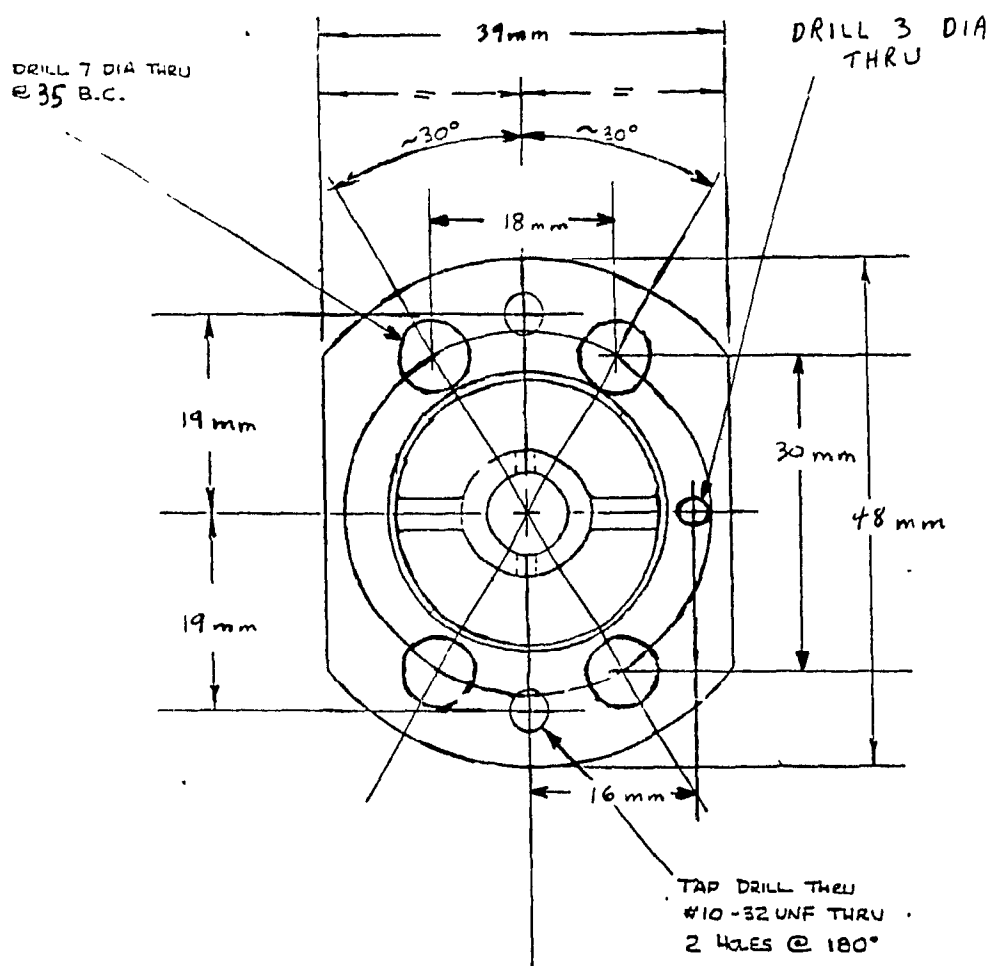
$$A = .64 \text{ mm } \begin{matrix} +0 \\ -.01 \end{matrix}$$

$$B = 17.02 \text{ mm } \begin{matrix} +0 \\ -.01 \end{matrix}$$

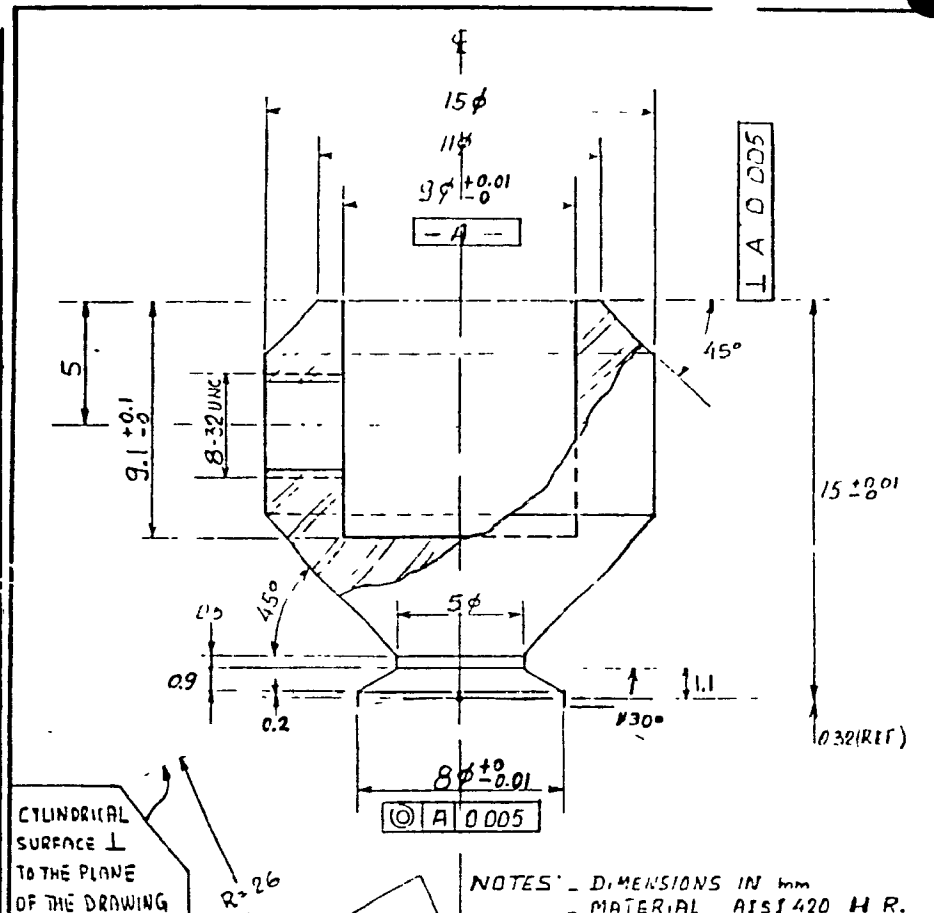
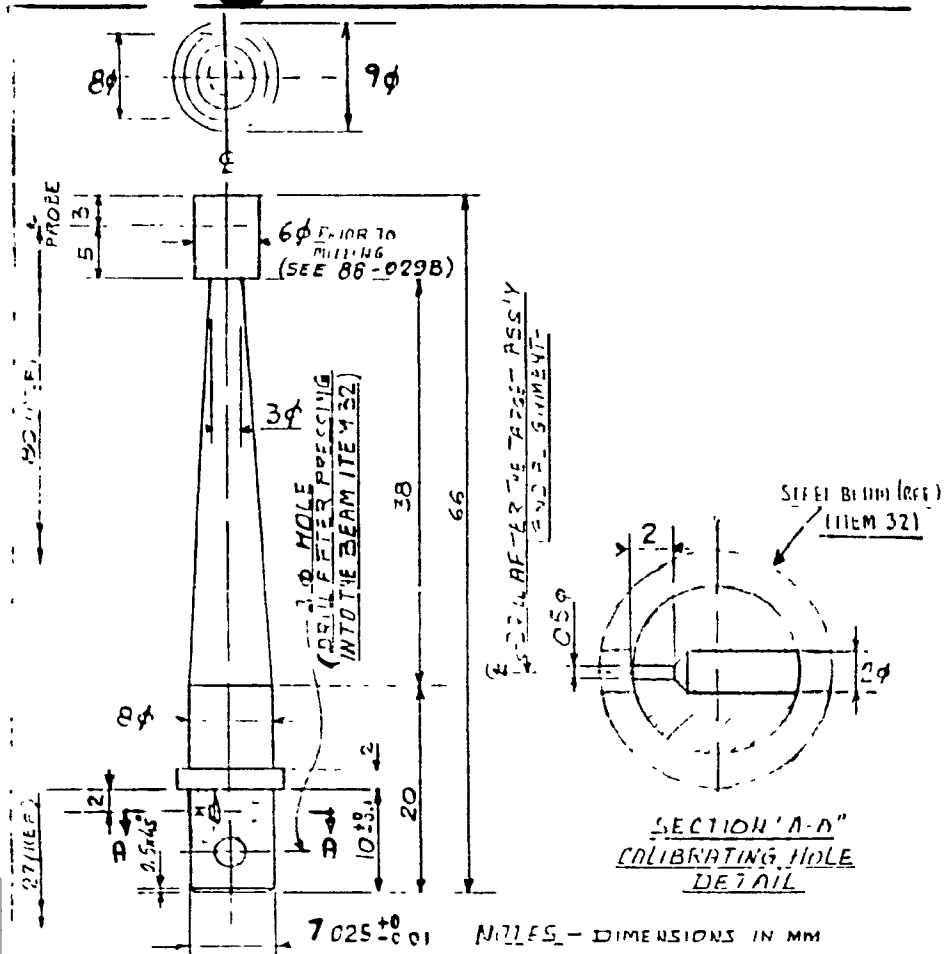
$$C = 1.06 \text{ mm } \begin{matrix} +0 \\ -.01 \end{matrix}$$

## A3.3 Shear Stress Transducer, Disk-Bar Top View

NOTE: MAT'L - AISI 420  
 SURFACE FINISH -  $(32 \mu\text{in}) \sqrt{0.8}$  U.N.  
 QTY - 1 REQ'D





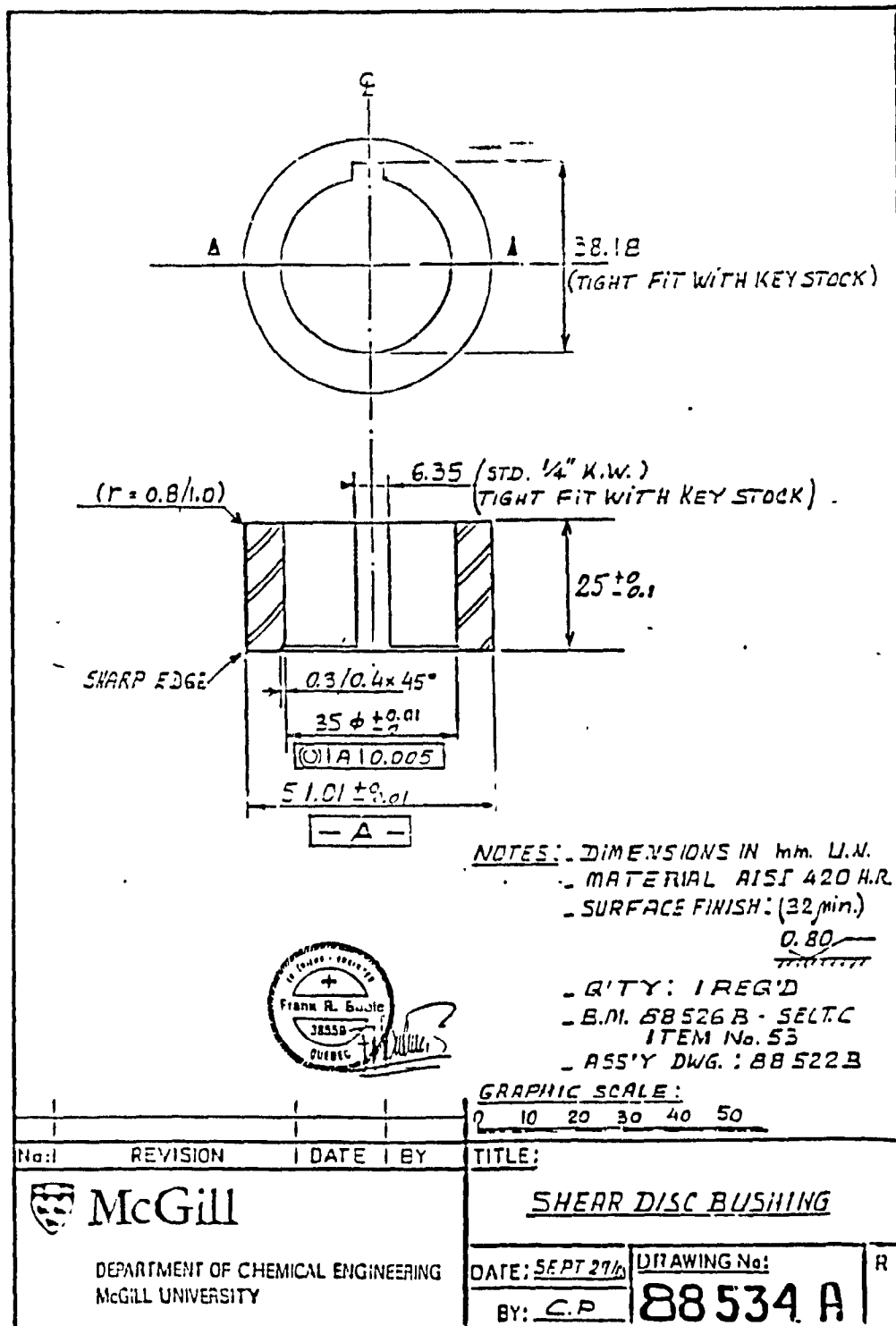


No.	REVISION	DATE	BY	TITLE
				TARGET
McGill				
DEPARTMENT OF CHEMICAL AND NUCLEAR ENGINEERING				
McGILL UNIVERSITY				
DATE:	DRAWING No:			
BY: CP	88031 A			

No.	REVISION	DATE	BY	TITLE
				ACTIVE FACE SST HEAD
McGill				
DEPARTMENT OF CHEMICAL AND NUCLEAR ENGINEERING				
McGILL UNIVERSITY				
DATE: FEB 78	DRAWING No:			
BY: CP	88027 A			

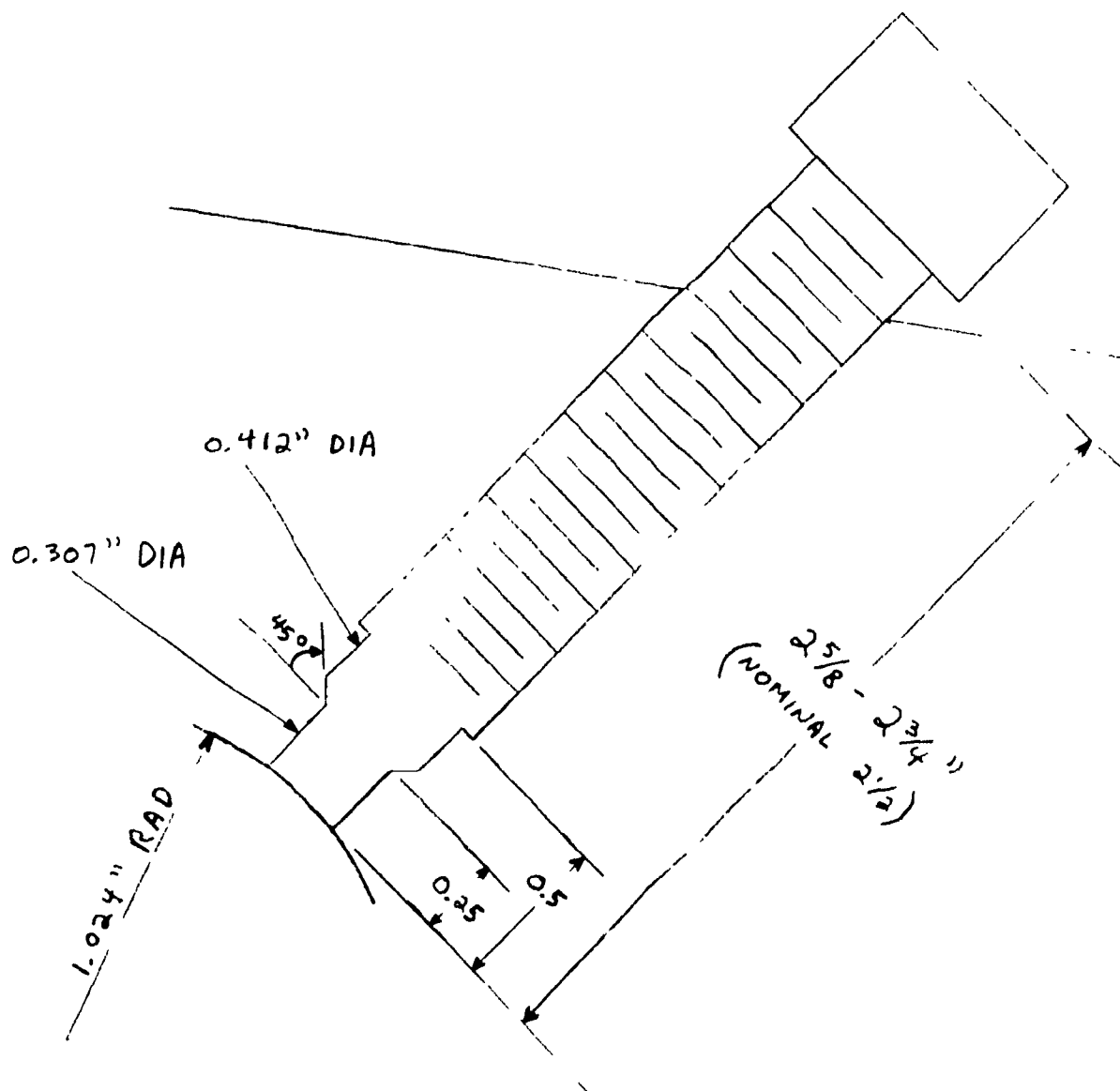
A3.5 Shear Stress Transducer, Active Face and Probe Target

## A3.6 Rheometer Drum



NOTE: BUSHING OUTER DIAMETER CHANGED  
FROM 50.01; AP

## A3.7 Gap Thermocouple

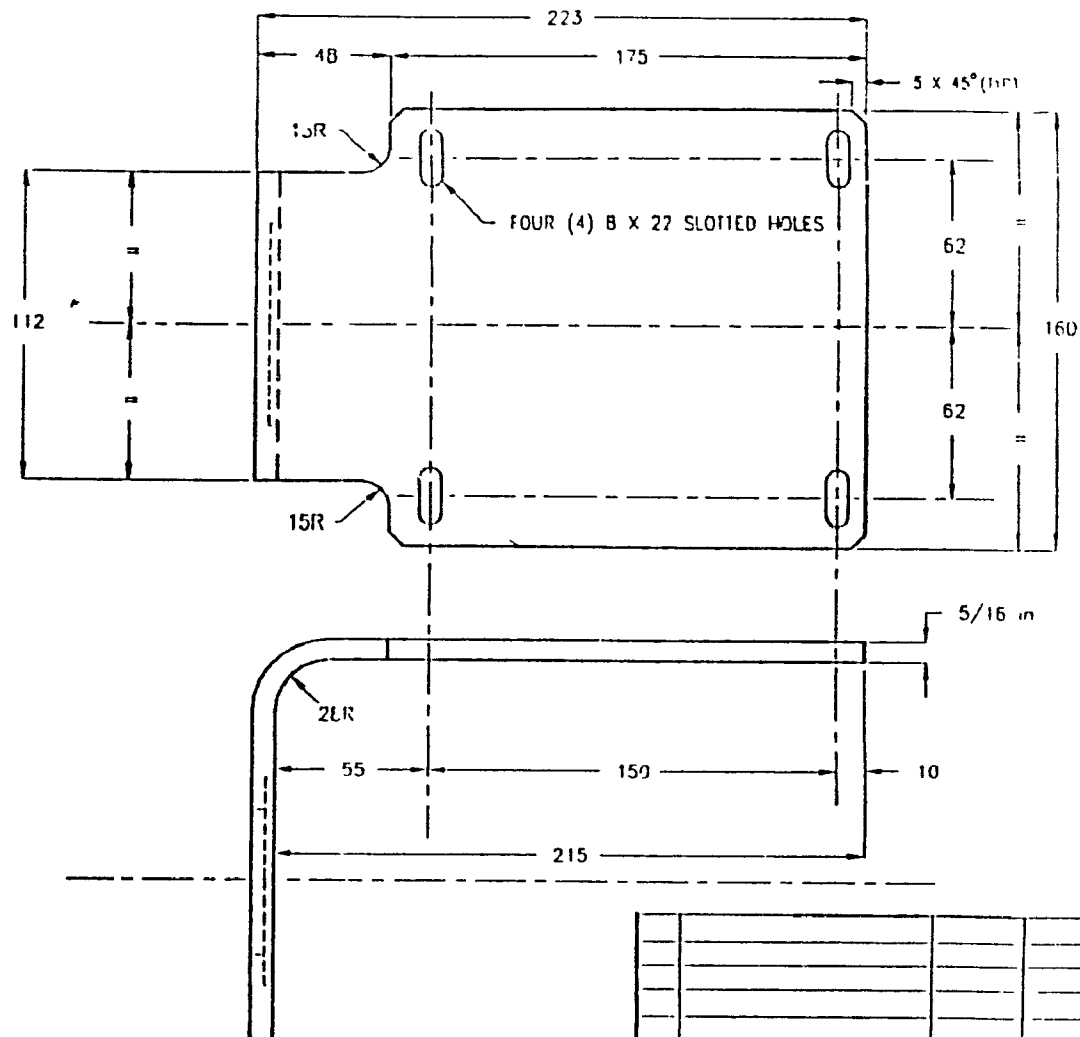
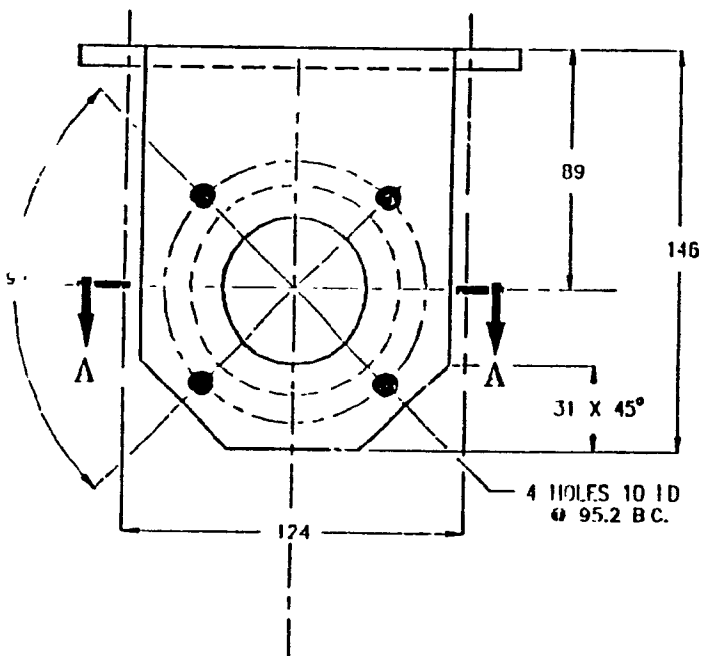
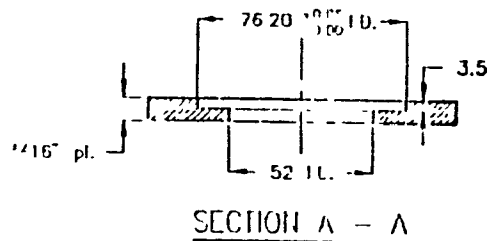
EXTRUD-O-COUPLE  
SPECIFICATIONS

## E - TYPE

PROBE FACE MUST BE CONTOURED  
TO A 1.024 INCH RADIUS ARC

TC SENSING TIP SHOULD EXTEND  
MAX 0.010 INCH FROM WALL





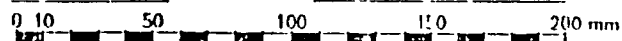
MATERIAL : H.R. STEEL  
ASIM A-36


QUANTITY : 1 REQ'D

ALL DIMENSIONS IN mm UN.

DRAWING OF MATERIAL 91 583 B

GRAPHIC SCALE:



No.	REVISION	DATE	BY
 <b>McGill</b> DEPT. OF CHEMICAL ENGINEERING MCGILL UNIVERSITY			
<b>TITLE:</b> D.C. MOTOR BRACKET FOR PROCESS RHEOMETER No. 345			
DATE: Oct 14/91		DRAWING No:	
BY: F.P. Dubuc		91 583 B	

88



UNABLE TO FILM MATERIAL ACCOMPANYING THIS THESIS ( I.E.  
DISKETTE(S), SLIDES, MICROFICHE, ETC...).

PLEASE CONTACT THE UNIVERSITY LIBRARY.

INCAPABLE DE MICROFILMER LE MATERIEL QUI ACCOMPAGNE CETTE THESE  
(EX. DISQUETTES, DIAPOSITIVES, MICROFICHE (S), ETC...).

VEUILLEZ CONTACTER LA BIBLIOTHEQUE DE L'UNIVERSITE.

NATIONAL LIBRARY OF CANADA  
CANADIAN THESES SERVICE

BIBLIOTHEQUE NATIONALE DU CANADA  
LE SERVICE DES THESES CANADIENNES

Floppy Disk:

System Identification and Control Programs      A. Pillo

DT-2801-A Data Acquisition and MACO 8000 Serial Communications  
Routines      B.I. Nelson